

Exact relations for dipolar quantum gases

Johannes Hofmann^{1,2,*} and Wilhelm Zwerger^{3,†}

¹*Department of Applied Mathematics and Theoretical Physics, University of Cambridge, Centre for Mathematical Sciences, Cambridge CB3 0WA, United Kingdom*

²*TCM Group, Cavendish Laboratory, University of Cambridge, Cambridge CB3 0HE, United Kingdom*

³*Technische Universität München, Physik Department, James-Franck-Strasse, 85748 Garching, Germany*

(Dated: July 29, 2020)

We establish that two-dimensional dipolar quantum gases admit a universal description, i.e., their thermodynamic properties are independent of details of the interaction at short distances. The only relevant parameters are the dipole length as well as the scattering length of the combined short-range plus dipolar interaction potential. We derive adiabatic relations that link the change in the thermodynamic potentials with respect to the scattering length and the dipole length to a generalized Tan contact parameter and a new dipolar contact, which involves an integral of a short-distance regularized pair distribution function. These two quantities determine the scale anomaly in the difference between pressure and energy density and also the internal energy in the presence of a harmonic confinement. For a weak transverse confinement, configurations with attractive interactions appear, which lead to a density wave instability beyond a critical strength of the dipolar interaction. We show that this instability may be understood in terms of a quantum analog of the Hansen-Verlet criterion for freezing of a classical fluid. Moreover, we argue that the experimentally observed supersolid phase beyond the instability is a superfluid version of the smectic A phase of liquid crystals. The associated hydrodynamic modes contain a propagating second sound mode which arises from the diffusive permeation mode of a normal smectic phase. In particular, the velocities of first and second sound provide a direct measure of both the effective layer compression modulus and the superfluid fraction.

I. INTRODUCTION

Interactions in ultracold gases are usually described in terms of the two-body scattering length a as a single parameter, which characterizes the complicated and in detail unknown microscopic interaction. Such a reduced description is possible because at low energies and densities, only two-particle s -wave collisions occur. Specifically, for low-energy scattering in potentials with a van der Waals tail, both the typical magnitude of the scattering length and the effective range $r_e \simeq \ell_{\text{vdW}}$ are of the order of the van der Waals length $\ell_{\text{vdW}} = (mC_6/\hbar^2)^{1/4}$, which is completely determined by the atomic mass m and the strength C_6 of the long-range interaction $-C_6/r^6$ [1]. The consequences of a description that only involves the s -wave scattering length for the associated many-body problem have been elucidated in the independent works by Tan [2–4] and by Zhang and Leggett [5] for two-component Fermi gases with a scattering length that is much larger than the typical interaction range r_e . They rely on the existence of a well-defined scaling limit $r_e \rightarrow 0$ at a fixed value of the scattering length a , for which the detailed form of the combined interatomic short-range and van der Waals potential becomes irrelevant. In particular, the zero-range limit leads to a set of exact relations for thermodynamic properties like the pressure or the energy of a trapped gas and also the behavior of

the momentum distribution $n(q)$ at large wave vectors q . Since these relations are based on operator identities, they hold for arbitrary phases of the many-body problem [6]. The temperature and the strength of the interaction enter only through a single parameter known as the contact [2–4]. The contact \mathcal{C} is a measure for two atoms to be in close proximity and sets the magnitude of the short-distance and short-time behavior of various correlation functions [7]. It remains finite even at infinite scattering length, a limit that may be reached intentionally by the use of Feshbach resonances [8]. Related strong coupling situations also appear accidentally in other areas of physics, for example, in the interaction between two ^4He atoms or in nuclear or high-energy physics, where the binding energies of the deuteron or the molecule $X(3872)$ of two charmed mesons are much smaller than the characteristic energy scale \hbar^2/mr_e^2 set by the range of the underlying interaction [9].

In this work, we establish that there exists an extended universal description for neutral atoms or molecules with a permanent magnetic or electric dipole moment, at least in the case of tight confinement into a two-dimensional configuration. Following the realization of a chromium BEC [10], the study of ultracold gases with dipolar interactions has become a major research field, in particular after both Bose and Fermi gases of dysprosium [11, 12] and erbium [13, 14] have been cooled into the deeply degenerate regime. In addition, stable quantum gases of molecules with a strong electric dipole moment have been created in RbCs [15, 16] and NaK [17]. More recently, considerable interest in dipolar gases has been triggered by the observation of supersolid phases, which appear in

* jbh38@cam.ac.uk

† zwerger@tum.de

weakly-confined two-dimensional BECs beyond a critical strength of the dipolar interaction [18–20]. The presence of attractively interacting dipoles in this case opens the possibility for an instability of the homogeneous superfluid into phases with spatial order. While there is no universal description of the short-distance correlations and thermodynamic properties in the limit of weak confinement, we derive exact results for the behavior of the static structure factor at large wave vectors. They allow to distinguish the transition to a phase with spatial order and the underlying onset of a roton minimum in the excitation spectrum from the classic example of ^4He . In addition, it is shown that the experimentally observed supersolid phase may be viewed as a superfluid version of the smectic A phase of liquid crystals. Exact results are derived for the associated hydrodynamic modes, which contain a second sound mode even at zero temperature. The velocities of longitudinal first and second sound turn out to be determined by only three low-energy parameters, which are the bulk and layer compression modulus and the superfluid fraction.

For dipolar gases, even with all dipoles aligned, the two-body interaction $-C_3 P_2(\cos\theta)/r^3$ depends on the angle θ between the direction of alignment and the relative separation. This anisotropic form of the interaction gives rise to a number of complications compared to the case of isotropic interactions with a van der Waals tail: Indeed, in three dimensions, a pure dipolar interaction gives rise to an ill-defined many-body problem due to its singular behavior at both short and long distances. At the two-body level, the spectrum of bound states is not bounded from below unless a non-universal short-distance cutoff is introduced [21]. Moreover, for scattering states, the phase shifts $\delta_l(k) = -\tilde{a}_l k + \mathcal{O}(k^2)$ start at linear order for all angular momentum channels. The associated effective scattering lengths $\tilde{a}_l \simeq \ell_d/l^2$ are determined by the characteristic dipolar length $\ell_d = mC_3/\hbar^2$ and they decay only slowly with increasing l [22]. Unlike the case of isotropic short-range interactions, the s -wave scattering length is therefore not sufficient to describe the two-body interaction at low energy. More generally, the s -wave scattering phase shift depends strongly on how the interaction is cut off at short distances and a universal scattering regime does not exist [23]. At the many-body level, the dipolar interaction decays too slowly to guarantee the independence of thermodynamic properties on the boundary conditions [24]. It is therefore far from evident that the thermodynamics and the behavior of correlation functions at large momenta in the many-body problem can be described in a universal manner that is insensitive to details of the interaction at short distances.

As will be shown below, a universal description of the many-body problem with dipolar interactions exists in the case of two dimensions, where the dipoles are tightly confined in a plane and aligned perpendicular to it. As

a result, the dipolar interaction

$$V_d(r) = \frac{d^2}{r^3} \quad (1)$$

is purely repulsive in addition to some unknown short-range potential. It decays sufficiently fast to give rise to proper thermodynamics with a finite value of the free energy per particle in the thermodynamic limit. In practice, the power-law form (1) is valid beyond a characteristic short-range cutoff r_e . As discussed by Büchler *et al.* [25], the effective range in the presence of a transverse confinement with oscillator length l_z is of order $r_e \simeq (l_z/\ell_d)^{4/5}\ell_d$. The existence of a proper zero-range scaling limit thus requires a tight transverse confinement with an associated length l_z considerably smaller than the dipolar length ℓ_d . In this limit, the many-body problem with dipolar interactions allows a universal description because, at the two-body level, the scattering states at low energy are fully characterized by a single parameter, namely the scattering length a_2 [defined formally in Eq. (4) below]. For a two-body interaction of the form (1) at arbitrary distance, this length coincides with the dipolar length $\ell_d = md^2/\hbar^2$ up to a numerical factor of order one, but in general with an additional short-range part of the interaction, the scattering length a_2 will be an independent parameter in addition to ℓ_d .

This paper is broadly split into two parts, where in the first part in Sec. II, we provide exact results for the strictly two-dimensional gas, and in the second part in Sec. III, we consider the weakly-confined system. In detail, the paper is structured as follows: We begin in Sec. II by considering the strictly two-dimensional dipolar gas where the confinement length l_z is much smaller than ℓ_d . Based on the solution of the associated two-body scattering problem in Sec. II A, we derive the short-distance properties of a many-particle wave function in Sec. II B. It involves a generalized version of the Tan contact, which determines the magnitude of the pair distribution function at short distances. In Section II C we discuss the related adiabatic relations and, in particular, define a new dipolar analog of the contact parameter. Moreover, using an extension to dipolar interactions of an approach due to Fisher and Hohenberg [26] to determine the equation of state of dilute Bose gases in two dimensions, explicit results for both contact parameters are derived in the low-density limit at zero temperature. The two independent contact parameters are linked to universal relations for the pressure and the virial theorem in Sec. II D. In Sec. II E we discuss the behavior of the momentum distribution and the static structure factor at large wave vectors. Based on previous numerical results for the ground state energy of a purely repulsive dipolar gas in both the low density fluid and the crystalline phase at high densities, quantitative results for the dipolar contact covering the full range of dimensionless coupling constants $\sqrt{n}\ell_d$ are presented in Section II F. In Section III we proceed to discuss the limit of weak transverse confinement, directly relevant to present experiments. It is shown that

the onset of a roton minimum in the excitation spectrum coincides with the quantum version of the Hansen-Verlet criterion, which determines the point at which the fluid becomes unstable towards a phase with broken translation symmetry. We derive exact results for the behavior of the static structure factor at large wave vectors which allow to distinguish the case of partially attractive interactions in weakly confined dipolar gases from the classic example of ^4He , where the interactions are dominantly repulsive. Moreover, in Sec. III B, we argue that the experimentally observed supersolid phase, exhibiting a mass density wave along a single direction, is a superfluid analog of a classical smectic A liquid crystal. We determine the resulting spectrum of both hydrodynamic and Goldstone modes along the direction of spatial order. The resulting first and second sound velocities depend on the bulk and layer compression modulus together with the superfluid fraction, which is smaller than one even at zero temperature. The paper is concluded by a summary in Sec. IV.

II. UNIVERSAL RELATIONS FOR THE STRICTLY TWO-DIMENSIONAL DIPOLAR GAS

In this section, we derive universal relations for a quantum Bose gas in two dimensions with dipole interactions. The many-body Hamiltonian of such a system with N particles is

$$\hat{H} = -\frac{\hbar^2}{2m} \sum_{i=1}^N \nabla_i^2 + \sum_{i<j} V(\mathbf{r}_i - \mathbf{r}_j). \quad (2)$$

Here, $V(\mathbf{r})$ is the complete effective interaction as truncated to motion in the plane. For separations $r > r_e$ larger than the effective range, the potential is assumed to be of the pure dipolar form given in Eq. (1) while for $r < r_e$, it changes to an unknown short-range dependence. In the following, we will consider the regime where both the scattering length a_2 associated with the full two-body interaction $V(\mathbf{r})$ and also the dipolar length ℓ_d are much larger than r_e (note that the scattering length in two-dimensions is denoted by a subscript a_2).

Throughout the paper, we consider a system of bosons, where only s -wave scattering is relevant at low energies. However, our results on the short-distance correlations and their connections to thermodynamic properties also hold for two-component Fermi gases with only minor modifications by factors of two. In fact, the latter problem is of relevance not only in the context of ultracold atoms but also arises in two-dimensional electron gases (2DEG). As discussed by Spivak and Kivelson [27], a realization of a two-component Fermi gas with dipolar interactions is provided by a 2DEG in a MOSFET device with a ground plane at a distance \tilde{d} . The interaction between the electrons in the 2DEG is then of a pure dipolar form at distances larger than \tilde{d} with an effective dipole moment $d_{\text{eff}}^2 = 4e^2\tilde{d}^2/\epsilon$, where ϵ is the dielectric constant of the

host semiconductor. Since the electrons are in an equal mixture of spin-up and spin-down state, scattering appears both in a relative singlet state associated with even angular momenta m or in relative triplet states which involves odd m . At low densities, where the Fermi wave vector k_F obeys $\ln(1/k_F\ell_d^{\text{eff}}) \gg k_F\ell_d^{\text{eff}}$, the s -wave contribution dominates and thus electron-electron interactions in relative triplet states become irrelevant. More generally, however, the scattering phase shifts $\delta_m(k) \sim k\ell_d$ associated with the long-range dipolar interaction in two dimensions are of the same order for arbitrary finite angular momenta $m \neq 0$ [28, 29]. A proper discussion of the electronic many-body problem at realistic densities, where $k_F\ell_d^{\text{eff}} \simeq (4/r_s)(\tilde{d}/a_B)^2$ is much larger than one, thus requires to include all possible values of m . (Here, $a_B = \hbar^2\epsilon/me^2$ is the effective Bohr radius and $r_s a_B = 1/\sqrt{\pi n}$ [30].) This is also the case for fermionic dipolar gases in a situation where only a single hyperfine state is present and thus all odd values of m contribute.

A. Two-body scattering

Before turning to the full many-body problem, we consider the two-body problem with the pure dipolar potential $V_d(r)$. The scattering wave function may be expanded in partial waves as $\psi(\mathbf{r}) = \frac{1}{\sqrt{\tilde{r}}} \sum_m e^{im\varphi} \phi_m(\tilde{r})$, where $m \in \mathbb{Z}$ is the integer angular momentum and φ the angle in the 2D plane. Introducing $\tilde{r} = r/\ell_d$ as the dimensionless radius and $\tilde{k} = k\ell_d$ as the corresponding relative wave vector, the Schrödinger equation for the relative motion reads

$$\left[-\frac{d^2}{d\tilde{r}^2} + \frac{m^2 - \frac{1}{4}}{\tilde{r}^2} + \frac{1}{\tilde{r}^3} - \tilde{k}^2 \right] \phi_m(\tilde{r}) = 0. \quad (3)$$

At large distances, the angular momentum contribution $\sim 1/\tilde{r}^2$ dominates. It is a peculiar property of scattering in two dimensions that this contribution gives rise to an attractive inverse square potential in the s -wave channel $m = 0$ while the standard repulsive behavior only applies for partial waves with $m \neq 0$. The low-energy scattering properties are therefore dominated by the s -wave solution. The associated scattering-phase shift $\delta_0(k)$ has a logarithmic dependence on momentum, which is characteristic for short-range interactions in two dimensions [31]. It is parametrized by a scattering length a_2 defined by the dominant first term in the effective range expansion

$$\cot \delta_0(k) = \frac{2}{\pi} \ln \frac{ka_2 e^{\gamma_E}}{2} - \frac{4\alpha}{\pi} (k\ell_d) \ln^2 ka_2 + \mathcal{O}(k), \quad (4)$$

where α is a positive numerical factor of order one. Note that for a dipolar interaction in two dimensions, the standard effective-range expansion does not hold [32]. The subleading term in the scattering phase shift (4) is therefore not of the usual form $\sim k^2$ but is non-analytic $\sim |k|$ in momentum and also contains an additional logarithmic factor [33]. Moreover, note that

the numerical factor $\exp(\gamma_E)/2$ in the leading contribution has been chosen such that no corrections of order k^0 are present. While this factor is often absorbed in the definition of a_2 (see, for example, Ref. [34]), our convention for the phase shift (4) ensures that the asymptotic form $\lim_{r \rightarrow \infty} \lim_{k \rightarrow 0} \phi(r) \sim \ln(r/a_2)$ of the two-body wave function at zero energy has no corrections of order $\mathcal{O}(r^0)$. The scattering states ϕ_m at small energies can be determined analytically in terms of modified Bessel functions [28]. For a pure dipolar interaction, one thus obtains $a_2^d = e^{2\gamma_E} \ell_d$ [28], as mentioned above. In order to deal with the realistic situation of an additional short-range part of the interaction at distances below the effective range r_e , it is sufficient to add the irregular solution in a pure dipolar potential with a prefactor $\ln(a_2/a_2^d)$. As a result, the two-body wave function is of the form

$$\phi(r) = 2K_0\left(\sqrt{\frac{4\ell_d}{r}}\right) - \ln\left(\frac{a_2}{a_2^d}\right) I_0\left(\sqrt{\frac{4\ell_d}{r}}\right). \quad (5)$$

At short distances $r \ll \ell_d$, the regular and irregular parts scale as an exponential with $(r/\ell_d)^{1/4} \exp \mp \sqrt{4\ell_d/r}$, which follows from a WKB approximation [35]. An important point to note is that the singular behavior $\sim 1/r^n$ with $n > 2$ of the dipolar potential at short distances [35, 36] does not allow to include the scattering length a_s of the bare short-range potential as a boundary condition as in the Bethe-Peierls approach. The relevant parameter is therefore the full scattering length a_2 of the combined short-range plus dipolar potential in addition to the dipolar length ℓ_d .

B. Pair distribution function and contact

A systematic method that connects the short-distance properties of a many-body system and two-body wave functions in vacuum is the operator product expansion (OPE) [6, 7, 37, 38]. For power-law interactions, this technique has been used previously in the Coulomb problem in Ref. [39]. Here, we follow a more intuitive approach that relies on the short-distance factorization of many-body wave functions. Specifically, we consider the pair distribution function $g(r)$, which describes the probability density of detecting pairs of particles separated by \mathbf{r} . Its formal expression

$$g(\mathbf{R}, \mathbf{r}) = \frac{N(N-1)}{n^2} \int d\mathbf{X} |\Psi(\mathbf{R} - \frac{\mathbf{r}}{2}, \mathbf{R} + \frac{\mathbf{r}}{2}, \mathbf{X})|^2 \quad (6)$$

contains the N -particle wave function Ψ in position space, where we introduce the short-hand $\mathbf{X} = (\mathbf{r}_3, \dots, \mathbf{r}_N)$ for those coordinates which are integrated over. We also use relative and centre-of-mass coordinates \mathbf{r} and \mathbf{R} for the first two particle coordinates. For a homogeneous system, there will be no dependence on \mathbf{R} . The basic assumption, which can be proven formally within the OPE, is that whenever two particle coordinates are close to each other, the wave function should

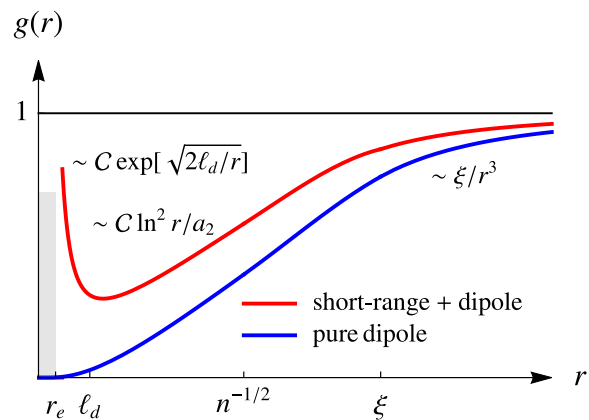


FIG. 1. Schematic plot of the pair distribution function for a system with combined dipole and short-range interaction (red line). For comparison, we also include the restricted case of a pure dipole interaction without a short-range part, for which $a_2 = e^{2\gamma_E} \ell_d$ (blue line). For distances that are small compared to the inter-particle separation $1/\sqrt{n}$ but still larger than the effective range r_e , the pair distribution function is universal [Eq. (8)], with a magnitude set by the contact (9).

approach the relative two-body solution up to a factor which is finite at $\mathbf{r} = 0$. The many-body wave function thus factorizes according to

$$\lim_{\mathbf{r}_1 \rightarrow \mathbf{r}_2} \Psi(\mathbf{r}_1, \mathbf{r}_2, \mathbf{X}) = \phi(\mathbf{r}) \mathcal{A}(\mathbf{R}; \mathbf{X}), \quad (7)$$

where $\phi(\mathbf{r})$ is defined in Eq. (5) and $\mathcal{A}(\mathbf{R}; \mathbf{X})$ is a remainder that does not depend on the relative coordinate \mathbf{r} . Using Eq. (7) in the definition of the pair distribution function gives the universal short-distance behavior

$$\lim_{r \rightarrow 0} n^2 g(\mathbf{R}, \mathbf{r}) = \frac{|\phi(r)|^2}{(2\pi)^2} \mathcal{C}(\mathbf{R}), \quad (8)$$

where we introduce the contact density $\mathcal{C}(\mathbf{R})$

$$\mathcal{C}(\mathbf{R}) = (2\pi)^2 N(N-1) \int d\mathbf{X} |\mathcal{A}(\mathbf{R}; \mathbf{X})|^2. \quad (9)$$

For a pure dipolar interaction $a_2 = a_2^d$, the pair distribution function is exponentially suppressed for $r \ll \ell_d$. In the actual relevant situation of an interaction which differs from the $1/r^3$ -behavior at short distances, however, $g(r)$ diverges exponentially near the origin, which is a consequence of the presence of the irregular solution I_0 in Eq. (5). The resulting overall form of the pair distribution function is illustrated in Fig. 1, where the continuous blue line denotes the case of a pure dipole interaction while the red line qualitatively describes the realistic situation of a combined dipole and short-range interaction. In observables that involve an integral over the pair distribution function, the exponential divergence of $g(r)$ at short distances must of course be cancelled, as will be shown explicitly in Eq. (16) below. In the limit of separations $r \gg \ell_d$ but still much smaller than the

average interparticle distance, the pair distribution function exhibits a logarithmic dependence $g(r) \sim \ln^2(r/a_2)$, which is the standard result for a two-dimensional system with finite scattering length [40, 41]. Note that this latter regime only exists in the low-density limit $\sqrt{n}\ell_d \ll 1$, where the dipole length is much smaller than the interparticle separation.

As indicated in Fig. 1, the pair distribution function has a universal form also at large distances: At zero temperature and for any compressible fluid phase, it approaches the asymptotic value one from below with an inverse cube power law

$$\lim_{r \rightarrow \infty} g(r) = 1 - \frac{\xi}{2\pi\sqrt{2}nr^3} + \dots \quad (10)$$

This dependence is a consequence of the non-analytic behavior $S(q \rightarrow 0) = |\mathbf{q}|\xi/\sqrt{2} + \dots$ of the static structure factor at small momentum that defines the characteristic length ξ . The large-distance result (10) then follows using the standard connection

$$S(\mathbf{q}) = 1 + n \int d\mathbf{r} e^{-i\mathbf{q}\cdot\mathbf{r}} (g(r) - 1) \quad (11)$$

between the static structure factor and the pair distribution function. A quite general upper bound on the length ξ has been derived by Price [42] using a combination of the f -sum rule and the compressibility sum rule. Defining $\bar{\kappa} = \partial n / \partial \mu$ as an effective compressibility, it reads

$$\xi \leq \hbar \sqrt{\frac{\bar{\kappa}}{2mn}}. \quad (12)$$

Within a single-mode approximation, where the density fluctuation spectrum at long wavelengths is exhausted by a single collective mode, the bound becomes an equality. In this case the length $\xi = \hbar/\sqrt{2}mc_s$ is uniquely determined by the speed of sound c_s .

C. Adiabatic relation

In the zero-range limit $a_2, \ell_d \gg r_e$, all information on the interaction is contained in the total scattering length a_2 and the dipolar length ℓ_d . One may therefore consider the change (here A denotes the area of the system)

$$d\Omega = -SdT - PdA - Nd\mu + X_a d(\ln a_2) + X_d d(\ln \ell_d), \quad (13)$$

of the grand canonical potential $\Omega = -PA$ in response to changes of these two parameters, which defines two extensive quantities X_a and X_d . They are the generalized forces conjugate to the variables $\ln a_2$ and $\ln \ell_d$ in $\Omega(T, A, \mu, a_2, \ell_d)$. In physical terms, X_a and X_d describe the work done on the system under changes in the scattering length or the dipole length at fixed temperature T , area A , and chemical potential μ . As shown in App. A,

these forces are related to the contact parameter defined in Eq. (9) in the following manner:

$$\frac{X_a}{A} = \left. \frac{\partial \varepsilon}{\partial (\ln a_2)} \right|_{\ell_d} = \frac{\hbar^2}{4\pi m} \mathcal{C} \quad (14)$$

$$\frac{X_d}{A} = \left. \frac{\partial \varepsilon}{\partial (\ln \ell_d)} \right|_{a_2} = \mathcal{D}, \quad (15)$$

where the partial derivatives of the energy density $\varepsilon = E/A$ are taken at fixed dipole length and scattering length, respectively, as well as at fixed entropy S , particle number N , and area A . In particular, the quantity \mathcal{D} is defined in terms of the pair distribution function as follows

$$\mathcal{D} = \frac{d^2}{2} \int d\mathbf{r} \frac{n^2 g(r) - \frac{|\phi(r)|^2}{(2\pi)^2} \mathcal{C}}{r^3}. \quad (16)$$

The first expression (14) is the standard Tan adiabatic theorem in two dimensions, generalized to the situation where the scattering length also includes the contribution from the dipolar interaction. It establishes the fact that the contact is finite and positive also in the presence of dipolar interactions. As a result, the energy is an increasing function of the scattering length [2]. The second relation is new and specific for gases with dipolar interactions. It defines a dipolar analog \mathcal{D} of the contact, which may be negative in general as shown below but is always finite. Indeed, the second term in the integral in Eq. (16) precisely cancels the short-distance divergence of the pair distribution function, Eq. (8), and thus renders the expression finite and independent of short-distance details. As will be shown in Eq. (28) below, the dipolar contact \mathcal{D} may be understood as a non-anomalous contribution measuring the deviation in the difference $P - \varepsilon$ between pressure and energy density due to the fact that a $1/r^3$ -interaction violates scale invariance explicitly. The adiabatic relations (14) and (15) are stated for a homogeneous system, however the extension to inhomogeneous or few-body states is straightforward. In this case, the pair distribution function $g(\mathbf{R}, \mathbf{r})$ and both contact densities $\mathcal{C}(\mathbf{R})$ as well as $\mathcal{D}(\mathbf{R})$ depend on the centre-of-mass coordinate \mathbf{R} . Upon integration over \mathbf{R} , they give rise to extensive values of X_a and X_d .

For a vanishing dipolar interaction, the full scattering length a_2 reduces to the two-dimensional scattering length of the short-range potential. The first adiabatic relation (14) then coincides with the standard adiabatic relation for bosons with short-range interactions [41]. Since the pair distribution function in this case behaves as

$$n^2 g(r)|_{d=0} = \frac{\ln^2(r/a_2)}{(2\pi)^2} \mathcal{C} + \mathcal{O}(r^2) \quad (17)$$

at short distances, the integral in Eq. (16) converges. The dipolar contact density \mathcal{D} thus vanishes as $\mathcal{O}(d^2)$ (with logarithmic corrections in na_2^2 , see below), as expected.

In the opposite limit of a negligible short-range contribution, the scattering length $a_2 = a_2^d \simeq \ell_d$ is fixed at the value obtained for a pure dipolar interaction. It is then no longer an independent thermodynamic variable separate from ℓ_d . As a result, the derivative with respect to ℓ_d gives a single adiabatic relation that is the sum of (14) and (15). Using the fact that the second term in the integral of Eq. (16) is finite for a pure dipolar interaction and cancels the contact term stemming from Eq. (14), one obtains

$$\tilde{\mathcal{D}} = \left. \frac{\partial \varepsilon}{\partial (\ln \ell_d)} \right|_{a_2=a_2^d} = \frac{d^2}{2} \int dr \frac{n^2 g(r)}{r^3}, \quad (18)$$

which is just the interaction energy density. This result can also be obtained directly using the Hellmann-Feynman theorem.

As emphasized above, the thermodynamic relations (14) and (15) hold for arbitrary states of the many-body problem, both at vanishing and at finite temperature. The calculation of the associated contact coefficients requires, however, a quantitative solution of the many-body problem, which is in general possible only numerically. Explicit results can be derived at zero temperature and low densities and probably also in the non-degenerate limit by means of a virial expansion, following the approach in Ref. [43] for the two- and three-body contacts of Bose gases with short-range interactions in three dimensions. In order to determine the contact densities \mathcal{C} and \mathcal{D} in the ground state at low densities, we use an approach due to Fisher and Hohenberg [26]. Based on results by Popov [44], they showed that for a quite general form of the two-body interaction, the dependence $\mu(n)$ of the chemical potential on the density n at small densities can be obtained from a perturbative solution of the implicit equation

$$\mu = n |t(0, 0, E = \mu)| = \frac{4\hbar^2 n/m}{|\cot \delta_0(k = \sqrt{m\mu/\hbar^2}) - i|}, \quad (19)$$

which involves the two-body T-matrix at vanishing total momentum evaluated at a finite energy $E = \mu$ in the center-of-mass frame.

In the presence of long-range dipolar interactions, the effective range expansion of the scattering phase shift in Eq. (4) gives rise to an equation of state at low densities of the form

$$n(\mu) = \frac{m\mu}{4\pi\hbar^2} \left\{ \frac{1}{\varepsilon(\mu)} + \frac{8I}{\pi} \varepsilon(\mu) \left(1 + \frac{\varepsilon(\mu)}{2} \right) + \alpha \ell_d \sqrt{\frac{m\mu}{\hbar^2}} \frac{1}{\varepsilon^2(\mu)} + \dots \right\}, \quad (20)$$

where $\varepsilon^{-1}(\mu) = \ln[4\hbar^2/(m\mu a_2^2 e^{2\gamma_E + 1})]$. The first term is the universal result for the chemical potential of a Bose gas with scattering length a_2 [26, 45]. In addition, we also include the leading and universal logarithmic corrections in the small parameter $\varepsilon(\mu) \ll 1$ which were

determined by Mora and Castin [46], with $I = 1.0005$ a numerical constant. These corrections are not contained in the Fisher-Hohenberg ansatz (19). In the ultra-low density limit, where $\varepsilon(\mu) \ll 1$, the equation of state only depends on the low-energy scattering length a_2 [47], and there is no separate dependence on the dipole length ℓ_d . The correction in Eq. (20) proportional to $\sqrt{n}\ell_d$ arises from the long-range nature of the dipolar interaction and becomes relevant beyond the limit of ultra-low densities. For example, for a pure dipolar gas with $a_2 = a_2^d$, this term will dominate over the Castin-Mora correction for $m\mu a_2^2/\hbar^2 \gtrsim 2 \cdot 10^{-4}$, corresponding to densities $\sqrt{n}\ell_d \gtrsim 10^{-3}$, which covers most of the relevant range in Fig. 3 below. This is indeed the point at which numerical calculations of a dipolar gas observe deviations from the equation of state of a Bose gas with short-range interactions [47]. The contact parameter can be determined from Eq. (19) or (20) using

$$nd\mu = dP - sdT + \frac{\hbar^2}{4\pi m} \mathcal{C} d(\ln a_2) + \mathcal{D} d(\ln \ell_d), \quad (21)$$

which follows from the definition of the contacts (13) and the Gibbs-Duhem relation. At low densities, the resulting contact

$$\mathcal{C}(a_2) = \left(\frac{4\pi n}{\ln[4e^{-2\gamma_E}/(na_2^2)]} \right)^2 + \dots \quad (22)$$

only involves the scattering length and — apart from the logarithmic factor — essentially vanishes with the square of the density. The dipolar contact arises from the contribution $\sim \ell_d$ in Eq. (20) and is given by

$$\mathcal{D} = -\frac{16\hbar^2 \alpha}{5m} \frac{\pi^{3/2} n^{5/2} \ell_d}{\ln^{1/2}[4e^{-2\gamma_E}/(na_2^2)]} + \dots \quad (23)$$

It is negative but vanishes faster with density than \mathcal{C} . A similar behavior is found in the two-body limit, where a bound state of the combined short-range plus dipolar interaction exists whenever $a_2 > a_2^d$ [48]. Using the adiabatic relation $dE/d\ln a_2 = \hbar^2 \mathcal{C}/(4\pi m)$, the resulting (integrated) contact $\mathcal{C}_{2\text{-body}} = 32\pi e^{-2\gamma_E}/a_2^2$ is positive while $\mathcal{D}_{2\text{-body}} = -\text{const} \cdot \hbar^2/(m\ell_d^3)$ is negative with a numerical prefactor const of order one. In the special case of a pure dipole interaction, where $a_2 = a_2^d \sim \ell_d$, only the dipolar contact remains. At low densities, it is determined by the perturbative result (22) apart from a trivial factor, i.e.,

$$\tilde{\mathcal{D}} = \frac{\hbar^2}{4\pi m} \mathcal{C}(a_2 = a_2^d). \quad (24)$$

D. Pressure relation and virial theorem

The adiabatic relations give rise to two additional exact expressions for the pressure in a uniform situation or the total energy in a harmonic trap. To derive these

relations, we write the grand canonical potential in dimensionless form

$$\begin{aligned} \Omega(T, \mu, A, 1/a, 1/\ell_d) \\ = k_B T \tilde{\Omega}\left(\frac{\mu}{k_B T}, \frac{\hbar^2/mA}{k_B T}, \frac{\hbar^2/ma_2^2}{k_B T}, \frac{\hbar^2/m\ell_d^2}{k_B T}\right). \end{aligned} \quad (25)$$

This relation implies the scaling law

$$\Omega(\lambda T, \lambda\mu, A/\lambda, \sqrt{\lambda}/a_2, \sqrt{\lambda}/\ell_d) = \lambda\Omega(T, \mu, A, 1/a_2, 1/\ell_d). \quad (26)$$

Taking the derivative of this expression with respect to λ and evaluating the result at $\lambda = 1$ gives

$$\left(T\frac{\partial}{\partial T} + \mu\frac{\partial}{\partial\mu} - A\frac{\partial}{\partial A} - \frac{1}{2}\frac{\partial}{\partial(\ln a_2)} - \frac{1}{2}\frac{\partial}{\partial(\ln \ell_d)}\right)\Omega = \Omega. \quad (27)$$

Using $(T\frac{\partial}{\partial T} + \mu\frac{\partial}{\partial\mu} - A\frac{\partial}{\partial A} - \Omega)\Omega = -TS - \mu N + PA - \Omega = PA - E$, we obtain a relation for the pressure:

$$P = \varepsilon + \frac{\hbar^2\mathcal{C}}{8\pi m} + \frac{\mathcal{D}}{2}. \quad (28)$$

For vanishing dipolar strength $d^2 \rightarrow 0$, the expression reduces to the 2D Tan relation [4, 49, 50]

$$P(\ell_d = 0) = \varepsilon + \frac{\hbar^2\mathcal{C}}{8\pi m}. \quad (29)$$

As noted above, the remaining contact term $\sim \mathcal{C}$ arises as an anomaly due to the fact that a zero range interaction in two dimensions is scale invariant only at the classical level. The invariance is broken in the quantum theory where the coupling constant becomes scale-dependent [50]. In the opposite limit of a dipolar interaction without a short-range part, the result

$$P(a_2 = a_2^d) = \varepsilon + \frac{\tilde{\mathcal{D}}}{2} \quad (30)$$

is equivalent to the virial theorem for a pure power law interaction $\sim 1/r^3$ since, as pointed out in Eq. (18), $\tilde{\mathcal{D}}$ is just the interaction energy density.

A different version of the virial theorem can be derived for dipolar gases that are confined by a harmonic radial trapping potential $V_{\text{ext}}(\mathbf{r}) = m\omega^2 r^2/2$ with frequency ω (for simplicity, we assume an isotropic trap, however the final result holds also in the anisotropic case). The associated grand canonical potential can then be written in dimensionless form as

$$\begin{aligned} \Omega(T, \mu, \omega, 1/a, 1/\ell_d) \\ = k_B T \tilde{\Omega}\left(\frac{\mu}{k_B T}, \frac{\hbar\omega}{k_B T}, \frac{\hbar^2/ma_2^2}{k_B T}, \frac{\hbar^2/m\ell_d^2}{k_B T}\right). \end{aligned} \quad (31)$$

A similar scaling analysis as above gives

$$\left(T\frac{\partial}{\partial T} + \mu\frac{\partial}{\partial\mu} + \omega\frac{\partial}{\partial\omega} - \frac{1}{2}\frac{\partial}{\partial(\ln a_2)} - \frac{1}{2}\frac{\partial}{\partial(\ln \ell_d)}\right)\Omega = \Omega. \quad (32)$$

Using $(T\frac{\partial}{\partial T} + \mu\frac{\partial}{\partial\mu} - 1)\Omega = -TS - \mu N - \Omega = -E$ and that the partial derivative of the grand canonical potential with respect to the trapping frequency is equal to the derivative of the energy (at fixed entropy), we obtain

$$\left(\omega\frac{\partial}{\partial\omega} - \frac{1}{2}\frac{\partial}{\partial(\ln a_2)} - \frac{1}{2}\frac{\partial}{\partial(\ln \ell_d)}\right)E = E. \quad (33)$$

Now, using $\omega\partial E/\partial\omega = 2\langle V_{\text{ext}}\rangle$, we obtain the virial theorem

$$E = 2\langle V_{\text{ext}}\rangle - \frac{\hbar^2}{8\pi m} \int_{\mathbf{R}} \mathcal{C}(\mathbf{R}) - \frac{1}{2} \int_{\mathbf{R}} \mathcal{D}(\mathbf{R}). \quad (34)$$

Again, the first two terms are the standard virial theorem for 2D quantum gases [4, 49–51]. For a pure dipolar interaction, the virial theorem reduces to

$$E = 2\langle V_{\text{ext}}\rangle - \frac{1}{2} \int_{\mathbf{R}} \tilde{\mathcal{D}}(\mathbf{R}). \quad (35)$$

This result can be compared with a virial theorem by Góral *et al.* [52] that was derived for trapped single-component dipolar Fermi gases in three dimensions in the semi-classical Thomas-Fermi limit. For spin-polarized fermions, there is no short-range contribution to the interaction energy and the virial theorem reported in Ref. [52] involves the 3D interaction energy associated with the long-range part $-C_3 P_2(\cos\theta)/r^3$ of the 3D dipolar interaction. Their result is consistent with Eq. (35) which applies in the presence of a tight confinement along the z -direction. Note, however, that the dipolar contact (18) is effectively evaluated with $g(r) \equiv 1$ in Ref. [52]. Due to trap-average, the $1/r^3$ -divergence of the dipole potential (1) at short distances is removed and thus the integral is finite despite neglecting short-range pair correlations. More generally, in three dimensions, the anisotropy of the interaction even in the case of oriented dipoles requires two independent scalar functions $g(r)$ and $g_D(r)$ to fully characterize the pair distribution function $g(1,2) = g(r) + g_D(r) \cdot 2P_2(\cos\theta)$, where θ is the angle between the separation vector \mathbf{r} and the dipole direction [53, 54]. This problem does not arise in two dimensions, where our general results (34) and (35) establish the virial theorem for arbitrary states of the many-body problem, including the realistic case of an interaction that differs from the dipolar form at short distances.

E. Momentum distribution and static structure factor

The short-distance factorization of the many-body wave function (7) also determines the high-momentum tails of various correlation functions, such as the momentum distribution and the static structure factor. Specifically, the momentum distribution is given by the Fourier

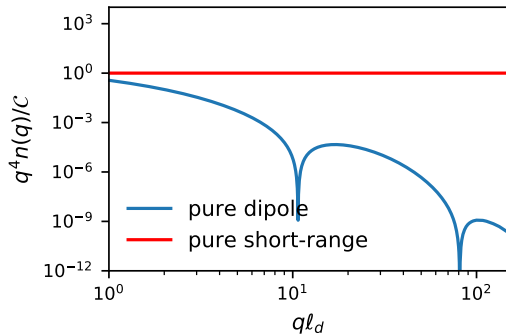


FIG. 2. Asymptotic high-momentum tail of the momentum distribution for a pure dipolar interaction as extracted from Eq. (37).

transform of the one-particle density matrix:

$$n(\mathbf{q}) = n \int d(\mathbf{r}_a, \mathbf{r}_b, \mathbf{r}_2, \dots, \mathbf{r}_N) e^{-i\mathbf{q} \cdot (\mathbf{r}_a - \mathbf{r}_b)} \Psi^*(\mathbf{r}_a, \mathbf{r}_2, \dots, \mathbf{r}_N) \Psi(\mathbf{r}_b, \mathbf{r}_2, \dots, \mathbf{r}_N), \quad (36)$$

which is a dimensionless quantity that is normalized to the density via $\int_{\mathbf{q}} n(\mathbf{q}) = n$. The dominant singularity at short distances arises from configurations in which both coordinates \mathbf{r}_a and \mathbf{r}_b approach any of the other $N - 1$ integration coordinates simultaneously. Using Eq. (7), this gives rise to the high-momentum behavior

$$\lim_{q \rightarrow \infty} n(\mathbf{q}) = \left| \int d\mathbf{r} e^{-i\mathbf{q} \cdot \mathbf{r}} \frac{\phi(r)}{2\pi} \right|^2 \mathcal{C}. \quad (37)$$

For quantum gases with short-range interactions, the two-body wave function at large momentum is $\phi(q) = 2\pi/q^2$. The momentum distribution thus exhibits a power-law \mathcal{C}/q^4 tail which in fact holds in any space dimension [3, 5, 40, 41, 49, 55, 56]. In the presence of dipolar interactions, this behavior remains valid for momenta $q\ell_d \ll 1$ since $\phi(r)$ may be replaced by the form $\phi(r) = \ln(r/a_2)$ valid in the regime $\ell_d \ll r \ll 1/\sqrt{n}$. For a pure dipolar gas, $\phi(r)$ becomes exponentially small at distances $r < \ell_d$. The momentum distribution is then exponentially suppressed at high momenta as well. Remarkably, it exhibits a nontrivial oscillatory structure arising from the Fourier transform of the modified Bessel function K_0 in Eq. (5). This is shown in Fig. (2) where the effective strength of the $1/q^4$ tail at high-momentum for the pure dipolar gas is depicted as a function of the dimensionless momentum $q\ell_d$ in a double-logarithmic plot. It exhibits a crossover from a power-law tail in the regime $\sqrt{n} \ll q \ll 1/\ell_d$ to exponential suppression for $q\ell_d \gg 1$. In practice, an observation of this peculiar behavior requires dipolar lengths ℓ_d of the order μm , which is significantly larger than the values which have been realized so far. In the presence of an additional short-range interaction, the exponential divergence of the two-body wave function (5) at short distances leads to a high-momentum

tail that depends strongly on a cutoff. In contrast to the thermodynamics, the behavior of the momentum distribution at large wave vectors is then no longer universal.

An analogous crossover is seen in the Fourier transform of the pair distribution function, which determines the static structure factor (11). The short-distance result for the pair distribution function in Eq. (8) implies the large-momentum behavior

$$\lim_{q \rightarrow \infty} [S(\mathbf{q}) - 1] = \frac{\mathcal{C}}{(2\pi)^2 n} \left(\int d\mathbf{r} e^{-i\mathbf{q} \cdot \mathbf{r}} |\phi(r)|^2 \right). \quad (38)$$

In an intermediate momentum region $\sqrt{n} \ll q \ll 1/\ell_d$, the logarithmic dependence of the pair distribution function gives rise to a power-law momentum tail

$$S(\mathbf{q}) - 1 = \frac{\mathcal{C}}{4\pi n q^2} \ln \frac{q a_2 e^{\gamma_E}}{2} + \dots, \quad (39)$$

which is modified by a logarithmic factor. For even larger momenta $q \gg 1/\ell_d$, this tail will be exponentially suppressed. The domain of validity $\sqrt{n} \ll q \ll 1/\ell_d$ for the expression (39) shows that the power-law decay is accessible only in the low-density regime $\sqrt{n}\ell_d \ll 1$, where the details of the long-range dipole potential are not important. The power-law tail (39) predicts a negative correction below $q < 2e^{-\gamma_E}/a_2$ while above that, the structure factor is larger than unity. Thus, a maximum appears at $\bar{q} = 2e^{1/2 - \gamma_E}/a_2$ which equals $\bar{q} \approx 0.58/\ell_d$ in the case of a pure dipolar interaction. Such a non-monotonic behavior has been observed in numerical calculations of the static structure factor by Astrakharchik *et al.* [57] close to the transition to a crystalline phase at high density $\sqrt{n}\ell_d \gtrsim 20$. This will be discussed in more detail in the following.

F. Numerical values of the dipolar contact

The result in Eq. (23) for the dipolar contact \mathcal{D} only covers the limit of ultra-low densities. In order to determine the contact quantitatively over a wider range — at least for a system with pure dipolar interactions, where $\mathcal{D} \rightarrow \tilde{\mathcal{D}}$ — we apply the adiabatic derivative (18) to the numerical results obtained in Ref. [57]. As shown in Fig. 3, the dimensionless dipolar contact increases monotonically with the ratio of the dipolar length ℓ_d and the average interparticle spacing, ranging over almost six orders of magnitude in a relevant range of densities.

In the low-density limit $\sqrt{n}\ell_d \ll 1$, the contact (24) follows the logarithmic dependence (22) derived in Sec. II C. In the opposite high-density limit $\sqrt{n}\ell_d \gtrsim 20$, the system forms a regular triangular lattice. The asymptotic dependence of the dipolar contact is then determined by the purely classical energy density of the crystal:

$$\tilde{\mathcal{D}}_{\text{crystal}} = \frac{n}{2} \sum_{\mathbf{R} \neq 0} \frac{d^2}{|\mathbf{R}|^3} = \frac{\hbar^2 n}{m \ell_d^2} (n \ell_d^2)^{3/2} \times \frac{1}{2} \sum_{\mathbf{R} \neq 0} \frac{1}{n^{3/2} |\mathbf{R}|^3}. \quad (40)$$

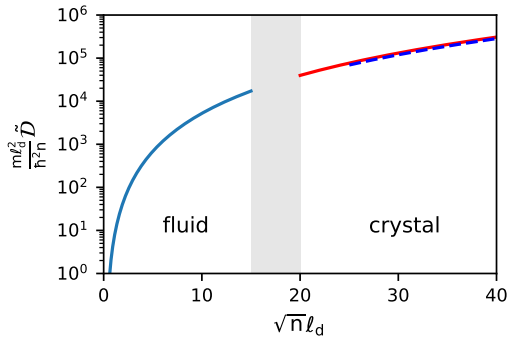


FIG. 3. Contact of a pure dipolar gas as extracted from the QMC calculations in Ref. [57] as a function of the dimensionless ratio of dipolar length and interparticle separation $\sqrt{n}l_d$. The blue line indicates the contact in the fluid phase and the red line in the crystalline phase, with an intermediate transition region between the two phases shown in gray. The exact result for the high-density limit is indicated by the blue dashed line.

The sum runs over the sites \mathbf{R} of a triangular lattice and the factor $1/2$ avoids double-counting. For a triangular lattice, the last purely numerical factor is 4.4462, which agrees with the corresponding constant $a_1 = 4.43(1)$ obtained numerically in Ref. [57]. In a square lattice, instead, one obtains a larger value $a_1^\square = 4.5168$ and thus a higher ground state energy. This is a reflection of the fact that for purely repulsive interactions the triangular lattice is the one with the lowest energy. Note that for a given density and strength d^2 of the dipolar interaction, \bar{D}_{crystal} is independent of \hbar . Quantum corrections to this purely classical energy arise from the zero point motion of the crystal. This leads to an additional contribution to the energy per particle of order $\tilde{\epsilon}_{\text{phon}} \simeq \hbar c_s / b \sim n^{5/4}$ because the sound velocity scales like $c_s \sim n^{3/4}$, while the lattice constant decreases like $b \sim 1/\sqrt{n}$ with density. The resulting quantum corrections to \bar{D}_{crystal} , which are of order $\mathcal{O}(n(nl_d)^{5/4})$, are quite small, however. Indeed, as shown in Fig. 3, the full result hardly differs from the dashed blue line representing the contribution (40) even in the regime close to the transition.

In the context of the fluid-to-crystal transition found numerically in Refs. [25, 57], two points merit further discussion. First of all, in two dimensions and in the presence of dipolar or even longer-range interactions, a direct first order transition from a fluid to a crystalline phase has been excluded by Spivak and Kivelson on quite general grounds [27, 58]. Indeed, such a transition requires a positive value of the surface tension. For interactions decaying like $V(r) \sim 1/r^n$ at large distances with $n \leq 3$, however, the fluctuation contributions to the surface tension in $d = 2$ become negative for large domain sizes [58]. As a result, one expects an inhomogeneous stripe or micro-emulsion phase intervening between the fluid and crystalline ground states. Such phases have been predicted for fast rotating gases in the presence

of dipolar interactions by Cooper *et al.* [59, 60]. In a non-rotating situation, where the projection to the lowest Landau level does not apply, they are difficult to resolve in numerical simulations, however, because in the special case of dipolar interactions the characteristic domain sizes are expected to be larger than the microscopic length scales ℓ_d or $1/\sqrt{n}$ by an exponentially large factor. To account for the presence of such intermediate phases, in Fig. 3 we have left open a finite interval in the vicinity of the critical dimensionless coupling $\sqrt{n}l_d$.

As a second point, we note that starting from a homogeneous fluid, the point of instability towards phases with a nontrivial modulation of the density may be inferred from a criterion which only involves knowledge of the static structure factor. In classical liquids, this is known as the Hansen-Verlet criterion. It states that freezing appears when the dominant first peak of the static structure factor reaches a critical value $S(q_0) = 2.85$ [61]. As discussed by Babadi *et al.* [62], a modified version of his criterion turns out to determine the limit of stability also for various two-dimensional quantum fluids at zero temperature. The associated critical value $S(q_0)$ is substantially lower than the classical Hansen-Verlet value, but does not change much with particle statistics or the specific form of the repulsive interactions. In the particular case of Bose fluids with dipolar interactions, the value extracted from the numerical results in Ref. [57] is $S(q_0) \simeq 1.7$ [62] (an even smaller value $S(q_0) \simeq 1.4$ applies for dominantly repulsive Bose fluids in $d = 3$ like ${}^4\text{He}$ [63]). In the following section, we will show that a criterion of this type also determines the position of an instability towards a ground state with a density wave which is found in dipolar gases in a situation where the transverse confinement length is much larger than the dipolar length and, therefore, the dipole part of the interaction is no longer purely repulsive.

III. EXACT RELATIONS FOR WEAKLY CONFINED DIPOLAR GASES

The results derived in the previous section apply for dipolar gases in the limit $r_e, l_z \ll a_2, \ell_d$, where the solution of the two-body problem takes the form (5) appropriate for scattering in two dimensions. In practice, such a strong confinement has not yet been reached. Indeed, typical dipolar lengths are below $100 a_B$ and are thus much smaller than the transverse confinement lengths on the order of $l_z \simeq 0.5 \mu\text{m}$ [64]. In such a case, the short-distance behavior is determined by a solution of the full three-dimensional Schrödinger equation in the presence of both a short-range and the dipolar potential:

$$V(\mathbf{r}) = V_{\text{sr}}(\mathbf{r}) + \frac{d^2}{r^3} \left(1 - \frac{3z^2}{r^2} \right) - \frac{8\pi d^2}{3} \delta^{(3)}(\mathbf{r}). \quad (41)$$

Here, the attractive delta-function term is specific to the case of magnetic point dipoles and ensures that $\text{div } \mathbf{B} \equiv 0$ holds globally [65]. As discussed in the introduction, the

associated scattering problem is not universal. Nevertheless, a number of exact results can be obtained for the weakly confined dipolar gas, where the motion along the confined z -direction is restricted to the lowest transverse single-particle eigenstate. This requires the chemical potential to obey the condition $\mu \ll \hbar\omega_z$ which excludes a high-density crystalline phase as discussed in the previous section.

The aim of this section is to show that the low-density system differs in key aspects from the dense quantum liquids commonly discussed in the literature. We begin in Sec. III A by demonstrating that the density-wave instability anticipated in early work on dipolar gases [66, 67] and recently observed by a number of groups [18–20] can be inferred from a quantum version of the Hansen-Verlet criterion for the static structure factor. In particular, we infer from this criterion that the region in parameter space where the homogeneous fluid shows a roton minimum is very limited, in contrast to dense quantum liquids like ^4He . Moreover, a universal relation for the high-momentum tail of the static structure factor suggests that the decay from the dominant peak at $q_0 \simeq 1/l_z$ to the asymptotic limit is monotonous, rather different from the non-monotonic behavior found for purely or dominantly repulsive systems like 2d gases with dipolar interactions [57] or superfluid ^4He [68]. Finally, in Sec. III B, we analyze the spectrum of hydrodynamic and Goldstone modes in a special case of the symmetry-broken supersolid phase which may be thought of as a superfluid version of a classical smectic A liquid crystal. Due to the broken translation symmetry along a single direction, the superfluid mass density tensor is anisotropic and there is a finite normal fluid density for longitudinal motion even at zero temperature. As a result, both first and second sound appears. The associated velocities are determined by a combination of the bulk and the layer compression modulus together with the superfluid fraction.

We begin with a brief discussion of the effective dipole interaction in the presence of a weak transverse confinement. The effective two-body interaction $V_{\text{dd}}(\mathbf{q})$ which results from projecting the three-dimensional dipole interaction (41) onto the lowest transverse oscillator level, has been determined by Fischer [69]. Its explicit form is given by

$$V_{\text{dd}}(\mathbf{q}) = -g_2^{\text{dd}} \sqrt{\frac{\pi}{2}} (ql_z) e^{q^2 l_z^2 / 2} \text{erfc}\left(\frac{ql_z}{\sqrt{2}}\right). \quad (42)$$

Here, following the notation in Ref. [34], we have introduced a coupling constant $g_2^{\text{dd}} = (\hbar^2/m)\tilde{g}_2^{\text{dd}}$ with a dimensionless factor $\tilde{g}_2^{\text{dd}} = \sqrt{8\pi}\ell_d/l_z$ for dipolar interactions, which is much less than one in practice. The effective interaction $V_{\text{dd}}(\mathbf{q})$ is always negative and approaches the constant value $-g_2^{\text{dd}}$ in the limit $ql_z \gg 1$. In physical terms, this describes attractive head-to-tail collisions between aligned dipoles with an effective 3D scattering length $-\ell_d$. Due to $\int V_{\text{dd}}^{\text{mag}}(\mathbf{r}) \equiv 0$, the projected dipolar interaction $V_{\text{dd}}(\mathbf{q}) \sim -2\pi d^2 q$ vanishes in the limit

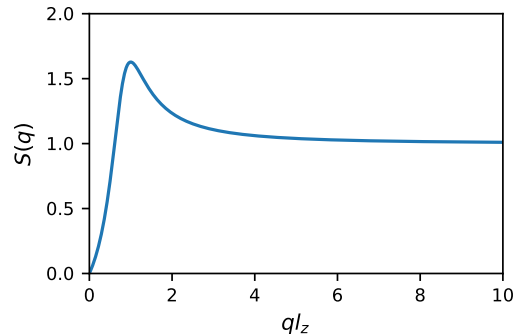


FIG. 4. Static structure factor of a weakly interacting Bose gas as predicted from Bogoliubov theory. Parameters are chosen such that a roton minimum just appears in the excitation spectrum and the dominant peak in the static structure factor at $ql_z \simeq 1.3$ has reached the critical Hansen-Verlet value 1.7.

$ql_z \ll 1$ with a linear slope, reflecting the repulsive d^2/r^3 potential at distances much larger than l_z .

The total momentum-dependent interaction $V_{\text{tot}}(\mathbf{q}) = g_2 + V_{\text{dd}}(\mathbf{q})$, which arises from the combination of a short-range part described by an associated scattering length a_s via $g_2 = (\hbar^2/m)\sqrt{8\pi}a_s/l_z$ [34] and the magnetic dipolar potential gives rise to a thermodynamically stable low-density gas provided that $a_s > 0$. In physical terms, this is equivalent to a positive value of the effective scattering length for head-to-head collisions between aligned dipoles. Note that this is a weaker condition compared to the case without a confining potential, where the effective scattering length $a_s^{\text{eff}} = a_s - \ell_d$ for head-to-tail collisions must be positive [70]. For quasi-2D systems, a_s^{eff} may become negative despite overall stability. It is the presence of attractively interacting dipoles in a weakly confined configuration with $l_z \gg \ell_d$ that opens the possibility for an instability of the homogeneous superfluid into phases with spatial order.

A. Static structure factor and Hansen-Verlet criterion

In the following, we will show that the critical strength of dipolar interactions where a density-wave instability occurs essentially coincides with the onset of a roton minimum in the excitation spectrum and may be understood in terms of a quantum version of the Hansen-Verlet criterion. The roton instability, where the excitation gap vanishes at some finite momentum q_0 , is thus preempted by a first order transition to a phase with a weak density modulation. In contrast to the case of ^4He , however, where the ground state changes from a superfluid to a normal solid at a critical pressure $p_c \simeq 25$ atm, the inhomogeneous phase of dipolar gases retains its superfluid properties and thus realizes an example of a supersolid [18–20]. This aspect will be discussed in more detail in the following section. Here, we will focus on the

Hansen-Verlet criterion and, moreover, provide exact results for the static structure factor at large momentum. This allows to distinguish the instability to a supersolid phase due to attractive interactions from the transition to an incompressible, commensurate crystal in the tightly confined limit discussed in the preceding section. It is important to note that the Hansen-Verlet criterion only determines the instability point of the homogeneous fluid phase. It does not fix the nature of the spatial order beyond the instability nor does it provide a microscopic description of the underlying first-order quantum phase transition. For the special case of weakly confined dipolar gases, various approaches to address the latter problem have been suggested, such as adding a repulsive three-body interaction on top of a Bogoliubov approximation, which may lead to either stripe or triangular spatial order [71]. In our present work, the problem of describing the transition to the supersolid phase is not addressed. Instead, we focus on exact results for the static structure factor at large momentum and on the hydrodynamic, low-energy description of an effectively one-dimensional supersolid phase beyond the instability.

As noted above, for dipolar interactions in two dimensions, the Hansen-Verlet criterion states that the dominant peak in the static structure factor reaches a critical value $S(q_0) \simeq 1.7$ at the transition to a phase with an inhomogeneous density. At the level of a Bogoliubov approximation, this criterion can be tested easily by noting that the resulting static structure factor

$$S_{\text{Bog}}(\mathbf{q}) = [1 + 2n_0 V_{\text{tot}}(\mathbf{q})/\varepsilon_q]^{-1/2} \quad (43)$$

is completely determined by the effective interaction and the condensate density n_0 ($\varepsilon_q = \hbar^2 q^2/2m$ is the single particle energy). Based on the expression (42) for the momentum dependent interaction, Fig. 4 shows the static structure factor at a dimensionless dipolar interaction strength $n_0 l_z^2 \tilde{g}_2^{\text{dd}} = 1$ and a negative effective short-range interaction $n_0 l_z^2 \tilde{g}_2^{\text{eff}} = -0.5$. This parameter regime corresponds to the onset of the roton minimum in the excitation spectrum which — within Bogoliubov theory — is given by the single-mode expression $E_q = \varepsilon_q/S(q)$. In Fig. 5, we show the associated stability diagram. Here, the blue line marks the roton instability, where the excitation energy reaches zero at finite momentum q_0 due to a formally divergent value of the static structure factor. Remarkably, the line where the excitation spectrum E_q starts to develop a roton minimum (orange line) as determined by Blakie *et al.* [72] essentially coincides with the Hansen-Verlet criterion $S(q_0) \simeq 1.7$ (green line). This suggests that — in contrast to the case of Helium 4 — a fluid phase with a well-developed roton minimum exists at most within a small range of parameter values: near the point where the roton minimum starts to develop, a first-order transition to an inhomogeneous phase appears. This appears in line with the experimental results obtained by Petter *et al.* [64], where a shallow minimum in the excitation spectrum near $ql_z \simeq 1.3$ is observed to decrease upon lowering the short-range scattering length

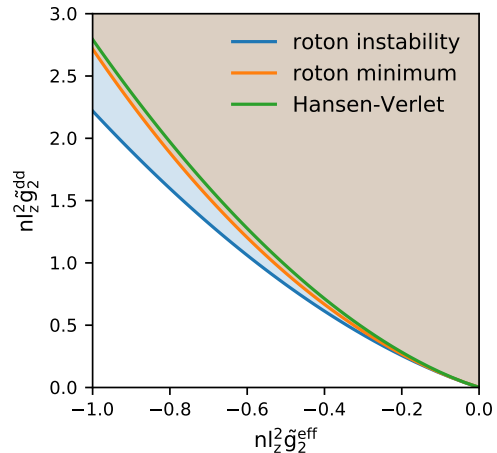


FIG. 5. Stability diagram of the weakly confined dipolar Bose gas as obtained within a Bogoliubov approximation. The blue line marks the region in parameter space in which the gas is stable (indicated by the blue and brown shaded regions). The orange line shows the onset of the roton minimum, and the green line marks the Hansen-Verlet criterion.

a_s , ending at a finite value $\omega_{\text{rot}} \simeq 0.5\omega_z$. An important point to note in this context is that the single-mode approximation for the excitation spectrum, which allows to extract a well-defined excitation energy for a given wave vector q , is valid in the relevant range $q \simeq 1/l_z$ only for confinement lengths l_z that are considerably larger than the effective healing length $\xi = \hbar/\sqrt{m\mu}$. At dimensionless coupling strengths $\tilde{g}_2^{\text{dd}} \simeq \ell_d/l_z$, however, this is incompatible with the condition $n\ell_d l_z \ll 1$ arising from the truncation $\mu \ll \hbar\omega_z$ to the lowest transverse eigenstate. In fact, as observed in Ref. [64], the excitation spectrum in the relevant range $q\xi \gtrsim 1$, covers a broad continuum at any given wave vector rather than a single sharp peak. This has been discussed in detail in Ref. [73] for the case of Bose gases with short range interactions in three dimensions. For tightly confined dipolar gases in 2D, it has been seen in numerical simulations by Mazzanti *et al.* [74].

In order to determine to which extent features in the static structure factor provide information about the nature of the instability towards inhomogeneous phases that remain valid beyond the Bogoliubov approximation, we first note that the associated high-momentum tail

$$\lim_{ql_z \gg 1} S_{\text{Bog}}(q) = 1 - \frac{4\sqrt{2\pi}n_2 a_s^{\text{eff}}}{l_z q^2} + \dots \quad (44)$$

is determined by the effective scattering length $a_s^{\text{eff}} = a_s - \ell_d$. The trivial asymptotic limit $S(q) = 1$ is thus approached from above provided $a_s^{\text{eff}} < 0$ is negative. It turns out, however, that the Gaussian approximation does not account for the correct asymptotic behavior of the static structure factor at large momentum. In fact, the tail of $S(q)$ for large in-plane momenta \mathbf{q} probes dipoles at lateral separations ρ that are much smaller

than the vertical displacement in the transverse direction. This can be seen from the definition of the static structure factor in terms of the pair distribution function

$$S(\mathbf{q}) = 1 + n_3 \int d\boldsymbol{\rho} e^{-i\mathbf{q}\cdot\boldsymbol{\rho}} \int dz (g(\boldsymbol{\rho}, z) - 1). \quad (45)$$

In the limit $ql_z \gg 1$, the dominant contribution comes from dipoles with lateral separation $|\boldsymbol{\rho}| \ll l_z$, which is averaged over the direction z of the dipoles. Quite different from the fluid-to-crystal transition discussed above, which is driven by purely repulsive interactions, the dipoles now may interact attractively. In particular, for distances below l_z the transverse confinement is not felt and the scattering problem is of a three-dimensional nature with an effective negative scattering length $a_s^{\text{eff}} < 0$, which describes the strength of head-to-tail collisions. For this parameter regime, the short-distance behavior of the pair distribution function is quite generally of the form [2]

$$g(\boldsymbol{\rho}, z) \sim \left(\frac{1}{r} - \frac{1}{a_s^{\text{eff}}} \right)^2. \quad (46)$$

Performing the Fourier transform in Eq. (45), the high-momentum tail of the structure factor is given by the exact result for three-dimensional systems [73]

$$S(q) - 1 \sim \frac{1}{8n_3q} \left(1 - \frac{4}{\pi q a_s^{\text{eff}}} + \dots \right). \quad (47)$$

This result holds for wave vectors larger than the inverse oscillator length $1/l_z$, yet smaller than inverse dipole length $1/\ell_d$, beyond which the details of the dipole interaction become important. With $l_z/\ell_d \simeq 150$ in current experiments [64], this is a broad window. Independent of the sign of a_s^{eff} , the static structure factor thus always approaches unity from above as $1/q$. For negative values $a_s^{\text{eff}} < 0$, which is the case relevant to current experiments [64, 75], also the subleading contribution is positive. As a result, the static structure factor exhibits a monotonic decay from its dominant peak at $q_0 l_z = \mathcal{O}(1)$ towards the limiting value one, as shown in Fig. 4. This is quite different from the situation found with purely repulsive interactions, where $S(q)$ exhibits both a minimum and a maximum at wave vectors beyond \sqrt{n} , see, for example, Ref. [57] and the discussion at the end of the previous section.

The Bogoliubov approximation (44), by contrast, fails to correctly describe the asymptotic form of the static structure factor (47) and only captures the subleading contribution $\sim 1/q^2$, missing the exact behavior (47) that always approaches unity from above. A similar situation is also found for Bose gases with pure short-range interactions and in the absence of a confinement [73].

B. Hydrodynamic and Goldstone modes in a superfluid smectic

In the following, we present exact results on the low-energy excitations of a particularly simple example of a superfluid phase with broken translation symmetry where the periodic modulation of the density is unidirectional. As mentioned above, such a phase has been observed experimentally [18–20]. It may be considered as a superfluid version of the smectic A phase of classical liquid crystals [76]. The results below are exact in a rather different sense than those of previous sections: they refer to the collective modes at long wavelengths and low energy. As emphasized by Martin *et al.* [77], the structure of such excitations is completely fixed by the number of conserved variables and that of broken symmetries. The superfluid smectic phase, where two separate symmetries — gauge invariance and translational invariance — are independently spontaneously broken, exhibits a distinct excitation spectrum with two independent Goldstone modes. Specifically, we focus on hydrodynamic modes propagating along the direction of the periodic modulation, which have recently been studied in experiments [78–80]. Besides the standard bulk sound mode, there is a separate second-sound type mode whose velocity is set by a combination of the layer compression modulus and the superfluid fraction. This is different from the individual cases of a smectic phase, where a secondary sound mode vanishes for propagation both along or perpendicular to the layer [76], or a homogeneous superfluid, where second sound is an entropy wave which becomes ill-defined at low temperatures.

In order to elucidate the similarities and differences between standard liquid crystals and the superfluid version of the smectic phase considered below, we start with the case where no superfluidity is present. Specifically, we consider a two-dimensional situation where the smectic order shows up as a weak periodic modulation

$$n_{\text{eq}}(\mathbf{r}) = \bar{n} + \sum_{l=1}^{\infty} n_l \cos(lq_0 y) \approx \bar{n} + n_1 \cos(q_0 y) + \dots \quad (48)$$

of the density along the y -direction with a fundamental reciprocal lattice vector q_0 . This type of ordering is observed for confined gases in the regime $l_z \gg \ell_d$ beyond the Hansen-Verlet bound for the critical value of the dipolar interaction. In the experiments, there is also an in-plane harmonic potential, which is very weak along the direction of ordering [20, 64]. For the following discussion, the in-plane trap frequencies $\omega_{x,y}$ are set to zero for simplicity. In particular, we assume translation invariance along the x -direction (i.e., transverse to the smectic order). Since our main focus lies on the longitudinal excitations, this assumption does not affect our conclusions below.

For a non-vanishing Fourier component $n_1 \neq 0$ in Eq. (48), translation invariance along y is broken. The associated new hydrodynamic variable is a scalar field

$u(x, y)$, which is called the layer phase [76]. It is defined by considering deviations from the equilibrium density (48) of the form

$$n(x, y) = \bar{n} + n_1 \cos[q_0 y - q_0 u(x, y)]. \quad (49)$$

In view of the four conserved quantities, which are particle number, momentum and energy combined with the single symmetry-breaking variable u , there must be five hydrodynamic modes. Only one of them is a Goldstone mode that counts twice in the hydrodynamic count because it is necessarily a propagating mode. As found by Martin *et al.* [77], the Goldstone mode of a smectic A liquid crystal is a transverse sound mode whose frequency $\omega_t(\mathbf{q}) \simeq \sqrt{B/\rho q^2} q_x q_y \sim \sin \psi \cos \psi$ depends on the angle ψ of the wave vector \mathbf{q} with the direction of the density order. Here, ρ is the total equilibrium mass density and B the layer compression modulus. It is defined by the elastic contribution $f_{\text{el}} = B(u')^2/2 + \dots$ to the free energy density associated with small longitudinal distortions $u' = \partial_y u$ of the smectic order [76]. Due to the peculiar angular dependence $c_t(\psi) \sim \sin \psi \cos \psi$ of the transverse sound velocity, this mode is absent for wave vectors \mathbf{q} along the y -direction. The spectrum of longitudinal excitations thus only contains a propagating bulk sound mode $\omega = \pm c_l q$ and three diffusive modes, one of which describes heat diffusion. The velocity

$$c_l^2 = \frac{K + B}{\rho}, \quad (50)$$

of the bulk sound mode is determined by the sum of the (isentropic) bulk modulus $K = \rho \partial p / \partial \rho|_{s, u'}$ and the layer compression modulus B [77]. For weak modulations of the density $n_1 \ll \bar{n}$, the bulk modulus dominates and thus the longitudinal sound velocity is essentially that of a fluid phase.

By mode counting at $q_x = 0$, there must be two further modes beyond heat diffusion. One is a transverse momentum diffusion mode with frequency $\omega = -i\nu q^2$, where ν is a kinematic viscosity [76]. The other one with frequency $\omega = -iD_p q^2$ is special to smectic A liquid crystals and is called the permeation mode [76]. It describes a diffusive process in which particles are exchanged between adjacent layers without changing the average periodic structure. The associated diffusion constant $D_p = \zeta B$ is determined by the layer compression modulus B and a dissipative coefficient ζ . The permeation mode may be viewed as an analog of vacancy diffusion, a process which gives rise to an independent hydrodynamic mode in any crystal [77]. As will be shown below, it is precisely the permeation mode in combination with the heat diffusion mode that turns into the Goldstone mode of the superfluid smectic phase, where exchange between the layers occurs in a reversible manner by non-dissipative, propagating mass currents.

For a description of the low-energy excitations of a superfluid smectic phase, the presence of superfluidity

needs to be included on a thermodynamic level by expressing the differential of the entropy density s

$$T ds = d\varepsilon - (\mu/m) d\rho - \mathbf{v}_n d\mathbf{g} - \mathbf{h} d(\nabla u) - \mathbf{j}_s d\mathbf{v}_s \quad (51)$$

as a function of the conserved variables energy density ε , mass density ρ , and momentum density $\mathbf{g} = \rho_n \mathbf{v}_n + \rho_s \mathbf{v}_s$ together with the gradient ∇u of the layer phase and the superfluid velocity \mathbf{v}_s , which characterize the two broken symmetries. The thermodynamic field

$$\mathbf{h} = \left. \frac{\partial f_{\text{el}}}{\partial(\nabla u)} \right|_{T, A, N, v_n, v_s} = B u' \mathbf{e}_y - K_1 \partial_x^3 u \mathbf{e}_x + \dots \quad (52)$$

conjugate to the gradient ∇u of the layer phase determines the elastic free energy of the smectic. Note that for longitudinal modes, only the layer compression modulus B plays a role. A different, Gaussian curvature type elasticity appears for excitations with a finite component q_x of the wave vector parallel to the layers. It involves the splay elastic constant K_1 [76], which is relevant for the dispersion of Goldstone modes in a Larkin-Ovchinnikov phase of imbalanced Fermi superfluids as discussed by Radzihovsky and Vishwanath [81, 82], see the discussion in Appendix C.

The conjugate variable to the momentum density \mathbf{g} is the normal velocity \mathbf{v}_n , which also appears in the superfluid mass current density $\mathbf{j}_s = \rho_s(\mathbf{v}_s - \mathbf{v}_n)$. Quite generally, for superfluids with an underlying periodic structure, the normal velocity $\mathbf{v}_n = \partial_t \mathbf{u}$ is determined by the time derivative of the displacement field \mathbf{u} . This relation — which is valid at the linearized level around equilibrium and is thus sufficient for the derivation of the hydrodynamic modes — may formally be derived as a consequence of Galilei invariance [83]. In particular, for hydrodynamic modes with wave vector \mathbf{q} along the y -direction, the associated normal velocity $v_{n,y} = \partial_t u$ is just the time derivative of the scalar layer phase variable u . Similar to the elastic constants B and K_1 , the superfluid and normal mass density tensors ρ_s and ρ_n which are constrained by $\rho_s + \rho_n = \rho \mathbf{1}$ are thermodynamic variables defined via \mathbf{j}_s as the conjugate field to \mathbf{v}_s . These relations are a straightforward tensor generalization of those from standard two-fluid hydrodynamics. For translation invariant fluids, the normal fluid density $\rho_n \sim T^{d+1} \mathbf{1}$ vanishes as the temperature approaches zero [26]. A rather different situation arises for a superfluid with smectic order, where the breaking of translation invariance along one of the directions gives rise to a finite value of the corresponding component $(\rho_n)_{yy} \simeq \rho \cdot (n_1/\bar{n})^2$ of the normal fluid density even at zero temperature. A strict lower bound for $(\rho_n)_{yy}$ follows from a variational argument due to Leggett [84], which is discussed in App. B.

The complete set of hydrodynamic modes in a superfluid smectic phase follows from the equations of motion for the conserved densities together with the two, effectively scalar, variables which describe the underlying broken symmetries. The latter are the superfluid velocity \mathbf{v}_s and the gradient of the layer phase ∇u , which are both

longitudinal vectors. Adding the particle density ρ , together with the momentum and energy densities \mathbf{g} and ε , the resulting equations of motion are given by

$$\partial_t \rho + \nabla \cdot \mathbf{g} = 0 \quad (53)$$

$$\partial_t g_i + \partial_j \pi_{ij} = 0 \quad (54)$$

$$\partial_t \varepsilon + \nabla \cdot \mathbf{j}^\varepsilon = 0 \quad (55)$$

$$\partial_t (\nabla u) - \nabla v_{n,y} = 0 \quad (56)$$

$$\partial_t \mathbf{v}_s + \nabla \mu / m = 0. \quad (57)$$

The first three equations (53)-(55) are continuity equations that link the time derivatives of the densities to the divergences of the momentum density \mathbf{g} , the stress tensor π_{ij} , and the energy current \mathbf{j}^ε , respectively. As already discussed above, Eq. (56) follows from Galilean invariance and expresses the fact that a constant shift along the direction of smectic order changes the layer phase by a constant [85]. Finally, Eq. (57) is the Josephson equation (neglecting a quadratic term in the velocities) that describes the dynamics of the superfluid phase.

From the differential of the entropy (51) and the dynamic equations (53)-(57), we obtain an expression for the material derivative $T(\partial_t s + \mathbf{v}_n \cdot \nabla s)$ of the entropy density that depends on spatial gradients ∇T , $\nabla \mu$, $\partial_i v_{n,j}$ and $\nabla \cdot \mathbf{j}_s$ of the thermodynamic forces. For the inviscid fluid considered here, there is no entropy production which implies a series of constitutive relations for the currents. To leading order in the velocities, they read:

$$\mathbf{g} = \rho \mathbf{v}_n + \mathbf{j}_s \quad (58)$$

$$\pi_{ji} = p \delta_{ij} - (h_i \delta_{j,y}) \quad (59)$$

$$\mathbf{j}_i^\varepsilon = (\varepsilon + p) v_{n,i} + \mu \mathbf{j}_{s,i} / m. \quad (60)$$

Compared to a simple fluid, at this level the superfluid order modifies the particle and energy current, while the smectic order modifies the stress tensor. In addition, as stated above, the thermodynamic forces \mathbf{j}_s and \mathbf{h} are linked to the velocities by $\mathbf{j}_s = \underline{\rho}_s (\mathbf{v}_s - \mathbf{v}_n)$ and $\mathbf{h} = B \partial_y u \mathbf{e}_y$.

The linearized hydrodynamic equations of motion are obtained by substituting the constitutive relations in the dynamic equations and expanding the thermodynamic forces to leading order in the hydrodynamic variables around equilibrium. For motion along the direction of the smectic order (here, the y -direction), the resulting equations only involve the yy component of the superfluid mass density tensor, which we denote by $\rho_s = \rho - \rho_n$ in the following. In this configuration, the transverse momentum degree of freedom decouples and gives rise to a diffusion mode. For the remaining degrees of freedom, we obtain the characteristic equation

$$\begin{pmatrix} -\omega/q & 1 & 0 & 0 & 0 \\ K/\rho & -\omega/q & 0 & 0 & -B \\ 0 & \tilde{s}T \frac{\rho_s}{\rho_n} & -\omega/q & -\rho \tilde{s}T \frac{\rho_s}{\rho_n} & 0 \\ K/\rho^2 & 0 & -\tilde{s}/\rho c_V & -\omega/q & 0 \\ 0 & 1/\rho_n & 0 & -\rho_s/\rho_n & -\omega/q \end{pmatrix} \begin{pmatrix} \delta \rho \\ g_L \\ \delta q \\ v_s \\ u' \end{pmatrix} = 0. \quad (61)$$

Here, ω is the frequency of the mode and q the associated longitudinal momentum. Moreover, we have introduced a heat current density variable $\delta q = \delta \varepsilon + \frac{\varepsilon + p}{\rho} \delta \rho$ where $\tilde{s} = s/\rho$ is the entropy per particle, and $c_V = \frac{T}{V \rho} \frac{\partial S}{\partial T} \Big|_\rho$ is the specific heat per particle at constant area. Apart from the transverse momentum diffusion mode mentioned above, Eq. (61) contains another diffusive zero mode with eigenvector $(\delta \rho, g_L, \delta q, v_s, u') = (-B\rho/K, 0, -B c_V / \tilde{s}, 0, 1)$. In the absence of superfluidity, this mode splits into two separate diffusion modes, one that describes heat diffusion, and one permeation mode that involves an interchange between the layer phase and the particle density. In the superfluid smectic phase, only the above combination remains, while an orthogonal complement will couple to the superfluid velocity and give rise to a propagating sound mode.

The determinant of Eq. (61), which determines the longitudinal hydrodynamic modes, reads

$$\omega^4 + \omega^2 q^2 \left[-\frac{K}{\rho} - \frac{B}{\rho_n} - \frac{\tilde{s}^2 T \rho_s}{c_V \rho_n} \right] + q^4 \left[\frac{BK \rho_s}{\rho^2 \rho_n} + \frac{\tilde{s}^2 T \rho_s}{c_V \rho_n} \frac{K - B}{\rho} \right] = 0. \quad (62)$$

Neglecting the terms of order $\tilde{s}^2 T / c_V$ at low temperatures, we obtain two undamped propagating modes $\omega = \pm c_{1,2} q$ with velocities

$$c_{1,2}^2 = \frac{K}{2\rho} + \frac{B}{2\rho_n} \pm \frac{1}{2} \left[\left(\frac{K}{\rho} + \frac{B}{\rho_n} \right)^2 - 4f_s \frac{KB}{\rho \rho_n} \right]^{1/2}. \quad (63)$$

The result turns out to be a special case of those obtained by Yoo and Dorsey [86] for the hydrodynamic modes of a crystalline supersolid. Indeed, Eq. (63) agrees with their Eqs. (48) and (49) if we identify the parameters $1/\chi \rightarrow K$ with the bulk compression modulus and $\lambda \rightarrow B$ with the layer compression modulus. Moreover, we do not include a strain-density coupling and thus $\gamma = 0$ in the notation of Ref. [86]. However, heat currents are neglected in Ref. [86] and therefore the contribution $\mathcal{O}(\tilde{s}^2 T / c_V)$ in Eq. (62) is absent. As briefly discussed in App. C, this is of relevance if one considers the hydrodynamic modes parallel to the layers which involve a conventional entropic second sound mode. In general, therefore, the hydrodynamic modes of a superfluid smectic phase differ from those of a crystalline supersolid. It is only in the specific case of purely longitudinal propagation that both systems behave in a similar manner. This also applies for the supersolid phase of a 2D gas with dipolar interactions, whose longitudinal modes have been determined numerically [87].

In crystalline supersolids, which have been studied in most of the literature so far, the superfluid fraction $f_s \ll 1$ is expected to be small. In this limit, the velocities reduce to $c_1^2 = (K + B)/\rho$ and $c_2^2 = f_s B/\rho$ if $K \gg B$. In particular, for $f_s = 0$, one recovers the normal state result from Eq. (50) together with $c_2 \equiv 0$, as expected. The superfluid smectic phase of interest here is closer to

the opposite limit, however, with a small normal fraction $f_n \ll 1$ on top of a dominant homogeneous superfluid. The contribution B/ρ_n in Eq. (63) then appears to diverge. This is not the case, however, since in the limit $f_n \simeq (n_1/\bar{n})^2 \rightarrow 0$ of a vanishing density modulation, the elastic constant B approaches zero too. The way it does has been discussed in the context of the nematic-to-smectic-A transition of normal liquid crystals [76]: Within a mean-field approximation, the layer compression modulus $B \sim |n_1|^2$ vanishes like the square of the order parameter n_1 . As a result, the ratio B/ρ_n turns out to be finite in the limit $n_1 \rightarrow 0$ where the smectic order disappears [88]. The ratio B/ρ_n is therefore a thermodynamic parameter that is finite in the superfluid smectic but vanishes in the homogeneous superfluid below the critical strength of the dipolar interaction. Using again that $K/\rho \gg B/\rho_n$ for a weak density modulation, it is straightforward to see that the velocities approach $c_1^2 = (K+B)/\rho$ and $c_2^2 = B/\rho_n$. The velocity of the compression mode is thus unchanged compared to the normal phase and is dominated by the bulk compression modulus K . The second sound mode, by contrast, only involves the ratio B/ρ_n of the layer compression modulus B and the normal fluid density. Physically, it describes the oscillatory motion of the periodic layer structure, which replaces the diffusive permeation mode of a normal smectic phase.

Experimentally, the existence of two independent modes $\omega_q = c_{1,2} q$ with a linear dispersion at small wave vectors has been observed in the excitation spectrum of the dipolar supersolid phase by Natale *et al.* [78]. The analytical results for the mode velocities in Eq. (63) thus allow to quantitatively determine the three parameters involved in the thermodynamic description of the superfluid smectic phase. Specifically, the bulk compression modulus K is fixed by the velocity $c_1^2 = K/\rho$ of first sound in the homogeneous superfluid before the density wave instability. It is expected to remain essentially unchanged in the supersolid phase, at least for small modulations $n_1 \ll \bar{n}$ of the density. A measurement of the two velocities in the superfluid smectic will then uniquely determine the two remaining parameters B/ρ_n and f_s , using, e.g., $c_1^2 + c_2^2 = K/\rho + B/\rho_n$ and $c_1^2 c_2^2 = f_s \cdot (K/\rho) (B/\rho_n)$. Beyond a direct measurement of the layer compression modulus B , this might allow to check the values of the superfluid fraction f_s extracted from the contrast $C = (n_{\max} - n_{\min})/(n_{\max} + n_{\min})$ of the density profiles in Ref. [75] via the Leggett bound.

IV. SUMMARY

In summary, we have shown that tightly confined dipolar gases admit a universal description that extends those developed by Tan and by Zhang and Leggett in the case of zero-range interactions. The description is based on only two experimentally tunable parameters, the two-dimensional scattering length and the dipolar

length scale. The associated adiabatic derivatives of the grand canonical potential define a generalized contact parameter and an additional dipolar analog of the contact. These two contact parameters determine thermodynamic relations such as the pressure of a homogenous system as well as the virial theorem in a trapped gas. Explicit results for both contacts have been given for zero temperature in the limit of low densities. In addition, we have discussed the behavior of the momentum distribution $n(q)$ and the static structure factor at large wave vectors. The standard C/q^4 -tail in $n(q)$ for short range interactions is replaced by a more complicated structure, exhibiting a characteristic minimum around $q\ell_d \simeq 10$.

The results presented in the first part of this paper apply in the limit of strong transverse confinement, a limit that has not yet been realized experimentally. A number of exact results, however, have also been derived for dipolar gases in a quasi-two-dimensional configuration. In particular, the high-momentum behavior of the static structure factor allows to distinguish the density wave instability in weakly confined dipolar gases from those in dense quantum liquids. Specifically, we show that in the former case one expects a monotonic decay from the dominant peak in the static structure factor towards the asymptotic value of unity. Moreover, we have shown that the quantum phase transition from a homogeneous fluid to a state with a finite density-wave modulation can be inferred from a quantum version of the classical Hansen-Verlet criterion for freezing. This criterion suggests that the appearance of a roton minimum with increasing strength of the dipole interaction is preempted by a first-order transition to a crystalline state. Finally, we have derived the hydrodynamic spectrum of a supersolid phase with a density wave along a single direction. This state may be viewed as a superfluid version of a classical smectic A liquid crystal. It has a highly anisotropic spectrum of modes which is entirely determined by the number of broken symmetries and a few thermodynamic parameters. In particular, the longitudinal excitations exhibit a second sound mode that remains well defined even at zero temperature. Together with the standard first sound, analytical results have been derived for the associated velocities. They may allow to experimentally determine both the superfluid fraction and the layer compression modulus as the characteristic elastic constant of a smectic phase.

ACKNOWLEDGMENTS

It is a pleasure to acknowledge a number of helpful comments by A. T. Dorsey, A. J. Leggett, S. Moroz, D. Petrov, L. Radzihovsky, A. Recati, and B. Spivak. This work is supported by Peterhouse, Cambridge (JH).

Appendix A: Derivation of the adiabatic relations

In this appendix, we present the derivation of the adiabatic relations (14) and (15) using the short-distance factorization of the many-body wave function (7). We begin by considering two energy eigenstates of the Hamiltonian (2) with different total scattering length and dipole strength, denoted by an index α and β , respectively: $\hat{H}_\alpha|\Psi_\alpha\rangle = E_\alpha|\Psi_\alpha\rangle$, and $\hat{H}_\beta|\Psi_\beta\rangle = E_\beta|\Psi_\beta\rangle$. The difference in energy is

$$\begin{aligned} (E_\alpha - E_\beta)\langle\Psi_\beta|\Psi_\alpha\rangle &= \langle\Psi_\alpha|\hat{H}\Psi_\beta\rangle - \langle\hat{H}\Psi_\alpha|\Psi_\beta\rangle \\ &= \int' d(\mathbf{r}_1, \mathbf{r}_2, \mathbf{X}) \left\{ -\frac{\hbar^2}{2m} \sum_{i=1}^N [\Psi_\alpha^* \nabla_i^2 \Psi_\beta - \Psi_\beta \nabla_i^2 \Psi_\alpha^*] \right. \\ &\quad \left. + \sum_{i < j}^N [V_\alpha(\mathbf{r}_i - \mathbf{r}_j) \Psi_\alpha^* \Psi_\beta - V_\beta(\mathbf{r}_i - \mathbf{r}_j) \Psi_\alpha \Psi_\beta^*] \right\}. \quad (\text{A1}) \end{aligned}$$

The prime on the integral denotes a restriction to a domain that excludes short-distance regions where two particle coordinates are close to each other, $|\mathbf{r}_i - \mathbf{r}_j| < \varepsilon$. The hypothesis is that if the system is universal, we are free to exclude this region in Eq. (A1) and then take the limit $\varepsilon \rightarrow 0$ such that the result is independent of ε . Applying the divergence theorem at the short-distance boundaries gives

$$\begin{aligned} (E_\alpha - E_\beta)\langle\Psi_\beta|\Psi_\alpha\rangle &= \frac{N(N-1)}{2} \int' d(\mathbf{R}, \mathbf{X}) \left\{ -\frac{2\pi\hbar^2\varepsilon}{m} \right. \\ &\quad \left. \times [\Psi_\alpha^* \frac{\partial\Psi_\beta}{\partial r} - \Psi_\beta \frac{\partial\Psi_\alpha^*}{\partial r}]_{r=\varepsilon} + \int_{\mathbf{r}}' [V_\alpha \Psi_\alpha^* \Psi_\beta - V_\beta \Psi_\alpha \Psi_\beta^*] \right\}. \quad (\text{A2}) \end{aligned}$$

For small variations $\delta a_2 = a_{2,\alpha} - a_{2,\beta}$ and $\delta \ell_d = \ell_{d,\alpha} - \ell_{d,\beta}$, the boundary term in Eq. (A2) is evaluated using Eq. (7) along with the relation

$$\varepsilon \left[\phi_\alpha^* \frac{\partial\phi_\beta}{\partial r} - \phi_\beta \frac{\partial\phi_\alpha^*}{\partial r} \right]_\varepsilon = -\frac{\delta a_2}{a_2} + \delta \ell_d \int_\varepsilon^\infty dr \frac{|\phi(r)|^2}{r^2}. \quad (\text{A3})$$

Substituting this result in Eq. (A2) and varying with respect to the universal parameters $\ln a_2$ and $\ln \ell_d$, we obtain the adiabatic relations for the energy density $\varepsilon = E/A$ stated in Eqs. (14) and (15).

Appendix B: Leggett bound on the superfluid fraction

An upper bound for the superfluid fraction f_s in a ground state with broken gauge and translation invariance, which only involves the microscopic density profile has been derived by Leggett [84]. In the special case of a purely one-dimensional configuration, Leggett's result states that

$$f_s = \frac{\rho_s}{\rho} \leq \frac{b}{\bar{n} \int_0^b dy/n(y)} \quad (\text{B1})$$

is bounded from above by an integral over a unit cell of the lattice (taken to be along the y -direction as in Eq. (48)) with lattice constant $b = 2\pi/q_0$ and average density \bar{n} . It is important to note that the bound does not rely on any commensurability condition: it applies both to a commensurate situation where the product $\bar{n}b = k$ of the average density and the lattice constant b is an integer $k = 1, 2, \dots$ or the generically incommensurate case associated with a weak mass-density wave, which is of relevance for the superfluid smectic. The bound becomes increasingly tight for densities that are strongly suppressed at intermediate points within a unit cell, as expected in a real crystal. In turn, superfluidity is favored if the density exhibits only small fluctuations around its average \bar{n} . Of course, the bound (B1) does not provide a sufficient criterion for superfluidity in a state with broken translation invariance: a finite value of the bound is still compatible with no superfluidity at all. What it shows, however, is that a ground state of bosons with non-uniform density necessarily has a finite normal fluid fraction.

Within a Gross-Pitaevskii description of the superfluid smectic phase (see, for example, Ref. [79]), it is assumed that the one-particle density operator $\hat{\rho}_1 = \sum_\alpha \lambda_\alpha^{(1)} |\psi_\alpha\rangle \langle\psi_\alpha|$ is dominated by a single macroscopic eigenvalue $\lambda_0^{(1)} \simeq N$. In the regime, where the ground state exhibits a weak density wave, the associated eigenfunction $\langle\mathbf{x}|\psi_0\rangle \sim 1 + \delta \cos(q_0 y) + \dots$ involves a small admixture of order $|\delta| \ll 1$ which breaks translation symmetry along the y -direction (in Ref. [75], this is called the sine ansatz). The resulting equilibrium density

$$n_{\text{eq}}(\mathbf{x}) = \langle\mathbf{x}|\hat{\rho}_1|\mathbf{x}\rangle \rightarrow \frac{\bar{n}}{(1 + \delta^2/2)} [1 + \delta \cos(q_0 y)]^2, \quad (\text{B2})$$

is then of the form assumed in Eq. (48) with $n_1/\bar{n} \simeq 2\delta$ to linear order in δ . For $|\delta| \geq 1$, the density (B2) vanishes quadratically at either one (for $|\delta| = 1$) or two different points within the unit cell, which leads to a divergent integral in the denominator of Eq. (B1). This is revealed by the special form

$$f_s \leq \frac{(1 - \delta^2)^{3/2}}{1 + \delta^2/2} \rightarrow 1 - 2\delta^2 \text{ for } \delta \rightarrow 0 \quad (\text{B3})$$

of the Leggett bound for the Gross-Pitaevskii state, which becomes increasingly tight for a large density modulation and is ill-defined for $|\delta| > 1$. As pointed out in the main text, the Leggett bound implies that the normal fluid fraction $f_n \geq 2\delta^2 + \dots$ in a state of the form (B2) is bounded from below by a finite value even at zero temperature. Unfortunately, the precise numerical factor connecting f_n with the square of the density modulation is not determined by this variational argument.

Appendix C: Hydrodynamic equations of a smectic A superfluid

In this appendix, we provide a few results on hydrodynamic modes of the smectic A superfluid beyond the purely longitudinal situation discussed in Sec. III B. We begin by collecting the dynamical equations for the hydrodynamic variables $(\delta\rho, g_L, g_T, \delta\varepsilon, v_s, \nabla u)$ (53)-(57) written in Fourier space for arbitrary angles ψ between the direction of propagation and the direction of smectic order. For this, it is helpful to decompose the current into a longitudinal and a transverse part defined by

$$g_L = \frac{q_x}{q} g_x + \frac{q_y}{q} g_y \quad (C1)$$

$$g_T = \frac{q_x}{q} g_y - \frac{q_y}{q} g_x. \quad (C2)$$

The continuity equation (53) can then be rewritten in terms of the longitudinal part of the current:

$$-\frac{\omega}{q} \delta\rho + g_L = 0. \quad (C3)$$

To rewrite the expression (54) for the longitudinal current, we introduce the longitudinal and transverse part of the conjugate field \mathbf{h} , which read with our choice (52) of the elastic free energy

$$h_{u,L} = u' B \cos^2 \psi \quad (C4)$$

$$h_{u,T} = u' B \cos \psi \sin \psi. \quad (C5)$$

Moreover, in expanding the pressure in terms of the hydrodynamic variables, we neglect its dependence on entropy, superfluid velocity, and layer phase gradient [89]. We obtain

$$\begin{aligned} -\frac{\omega}{q} g_L + p - h_{u,L} \cos \psi \\ = -\frac{\omega}{q} g_L + [K \delta\rho - B \cos^3 \psi u'] = 0. \end{aligned} \quad (C6)$$

Likewise, the equation (54) for the transverse current component becomes

$$\begin{aligned} -\frac{\omega}{q} g_T - h_{u,L} \sin \psi \\ = -\frac{\omega}{q} g_T - B \cos^2 \psi \sin \psi u' = 0. \end{aligned} \quad (C7)$$

In order to derive an expression for the energy density (55), we use the continuity equation (C3), the constitutive relations for the current (58), as well as the expression for the pressure,

$$-p = \varepsilon - sT - \mu\rho - \mathbf{j} \cdot \mathbf{v}_n, \quad (C8)$$

which has the thermodynamic differential

$$dp = sdT + \rho d\mu + \mathbf{j} \cdot d\mathbf{v}_n - \mathbf{j}_s \cdot d\mathbf{v}_s - \mathbf{h} \cdot d(\nabla u). \quad (C9)$$

In addition, we use the decomposition of the superfluid current

$$\begin{aligned} j_{s,L} = -g_L \left[\frac{\rho_s^y}{\rho_n^y} \cos^2 \psi + \frac{\rho_s^x}{\rho_n^x} \sin^2 \psi \right] \\ - g_T \cos \psi \sin \psi \left[\frac{\rho_s^y}{\rho_n^y} - \frac{\rho_s^x}{\rho_n^x} \right] + \rho v_s \left[\frac{\rho_s^y}{\rho_n^y} \cos^2 \psi + \frac{\rho_s^x}{\rho_n^x} \sin^2 \psi \right] \end{aligned} \quad (C10)$$

$$\begin{aligned} j_{s,T} = g_L \cos \psi \sin \psi \left[\frac{\rho_s^x}{\rho_n^x} - \frac{\rho_s^y}{\rho_n^y} \right] \\ - g_T \left[\frac{\rho_s^y}{\rho_n^y} \sin^2 \psi + \frac{\rho_s^x}{\rho_n^x} \cos^2 \psi \right] + \rho v_s \cos \psi \sin \psi \left[\frac{\rho_s^y}{\rho_n^y} - \frac{\rho_s^x}{\rho_n^x} \right] \end{aligned} \quad (C11)$$

in the definition (60) of the energy current. Here, we abbreviate the xx and the yy components of the superfluid and normal tensor by a superscript x and y , respectively. Collecting all terms, we obtain

$$\begin{aligned} -\frac{\omega}{q} \delta\varepsilon + \hat{\mathbf{q}} \cdot \mathbf{j}^\varepsilon = -\frac{\omega}{q} \delta q - \tilde{s}T \left\{ g_T \cos \psi \sin \psi \left[\frac{\rho_s^x}{\rho_n^x} - \frac{\rho_s^y}{\rho_n^y} \right] \right. \\ \left. - g_L \left[\frac{\rho_s^y}{\rho_n^y} \cos^2 \psi + \frac{\rho_s^x}{\rho_n^x} \sin^2 \psi \right] \right. \\ \left. + \rho v_s \left[\frac{\rho_s^y}{\rho_n^y} \cos^2 \psi + \frac{\rho_s^x}{\rho_n^x} \sin^2 \psi \right] \right\} = 0. \end{aligned} \quad (C12)$$

In a similar way, the equation for the gradient of the layer phase becomes

$$\begin{aligned} -\frac{\omega}{q} u + v_{n,y} \\ = -\frac{\omega}{q} u + \frac{\cos \psi}{\rho} (g_T - j_{s,T}) + \frac{\sin \psi}{\rho} (g_L - j_{s,L}) \\ = -\frac{\omega}{q} u + g_L \frac{\cos \psi}{\rho_n^y} + g_T \frac{\sin \psi}{\rho_n^y} - v_s \frac{\rho_s^y}{\rho_n^y} \cos \psi = 0. \end{aligned} \quad (C13)$$

To simplify the equation (57) for the superfluid velocity, we use the differential (C9) to leading order in the velocities in order to replace $d\mu$:

$$-\frac{\omega}{q} v_s + \frac{1}{\rho} \frac{\partial p}{\partial \rho} \Big|_{\tilde{s}, v_s, u'} \delta\rho - \frac{\tilde{s}}{\rho c_V} \delta q = 0. \quad (C14)$$

Collecting the equations (C3), (C6), (C7), (C13), and (C14) gives the characteristic equation (abbreviating $c = \cos \psi$ and $s = \sin \psi$)

$$\begin{pmatrix} -\omega/q & 1 & 0 & 0 & 0 & 0 \\ K/\rho & -\omega/q & 0 & 0 & 0 & -Bc^3 \\ 0 & 0 & -\omega/q & 0 & 0 & -Bsc^2 \\ 0 & \tilde{s}T\left[\frac{\rho_s^y}{\rho_n^y}c^2 + \frac{\rho_s^x}{\rho_n^x}s^2\right] & \tilde{s}Tsc\left[\frac{\rho_s^y}{\rho_n^y} - \frac{\rho_s^x}{\rho_n^x}\right] & -\omega/q & -\rho\tilde{s}T\left[\frac{\rho_s^y}{\rho_n^y}c^2 + \frac{\rho_s^x}{\rho_n^x}s^2\right] & 0 \\ K/\rho^2 & 0 & 0 & -\tilde{s}/\rho_{CV} & -\omega/q & 0 \\ 0 & c/\rho_n^y & s/\rho_n^y & 0 & -\rho_s^y c/\rho_n^y & -\omega/q \end{pmatrix} \begin{pmatrix} \delta\rho \\ g_L \\ g_T \\ \delta q \\ v_s \\ u' \end{pmatrix} = 0. \quad (\text{C15})$$

The associated characteristic determinant is

$$\begin{aligned} & \omega^6 + \omega^4 q^2 \left[-\frac{K}{\rho} - \frac{B}{\rho_n^y} c^2 - \frac{\tilde{s}^2 T}{c_V} \left(\frac{\rho_s^y}{\rho_n^y} c^2 + \frac{\rho_s^x}{\rho_n^x} s^2 \right) \right] \\ & + \omega^2 q^4 \left[\frac{BK}{\rho^2} c^2 \left(\frac{\rho}{\rho_n^y} c^2 + \frac{\rho_s^y}{\rho_n^y} s^2 \right) \right. \\ & + \left. \frac{\tilde{s}^2 T}{\rho_{CV}} \left(K \left(\frac{\rho_s^y}{\rho_n^y} c^2 + \frac{\rho_s^x}{\rho_n^x} s^2 \right) + Bc^2 \left(\frac{\rho_s^y}{\rho_n^y} c^2 + \frac{\rho}{\rho_n^y} \frac{\rho_s^x}{\rho_n^x} s^2 \right) \right) \right] \\ & + q^6 \left[-\frac{BK}{\rho\rho_n^x} \frac{\tilde{s}^2 T}{c_V} c^2 s^2 \left(\frac{\rho_s^y}{\rho_n^y} c^2 + \frac{\rho_s^x}{\rho_n^x} s^2 \right) \right] = 0. \quad (\text{C16}) \end{aligned}$$

In general, there are three distinct propagating modes. One of them is a generalized transverse sound mode $\omega_t(\mathbf{q})$, which is the Goldstone mode associated with smectic order found by Martin *et al.* [77]. As noted in Sec. III B, its velocity vanishes in the special case of purely parallel and perpendicular propagation. Formally, this is due to the fact that the last term of the characteristic polynomial vanishes, giving rise to only two sound modes plus two diffusive ones. For propagation in the longitudinal direction ($c = 1$ and $s = 0$), the matrix (C15) reduces to the expression (61) in the main text (the transverse current component decouples and can be omitted). In the opposite limit $\psi \rightarrow \pi/2$, where propagation is parallel to the smectic layers, we find instead

$$\omega^4 + \omega^2 q^2 \left[-\frac{K}{\rho} - \frac{\tilde{s}^2 T}{c_V} \frac{\rho_s^x}{\rho_n^x} \right] + q^4 \left[\frac{K}{\rho} \frac{\tilde{s}^2 T}{c_V} \frac{\rho_s^x}{\rho_n^x} \right] = 0. \quad (\text{C17})$$

Note that there is no dependence on B , ρ_s^y , and ρ_n^y . We find the standard first and second sound modes with speed

$$c_1^2(\psi = \pi/2) = \frac{K}{\rho} \quad (\text{C18})$$

$$c_2^2(\psi = \pi/2) = \frac{\tilde{s}^2 T}{c_V} \frac{\rho_s^x}{\rho_n^x}, \quad (\text{C19})$$

which is as expected: in the special case of propagation along the smectic layers, the density wave structure does not affect the hydrodynamic modes, which are the same as for a homogenous superfluid. Since the normal fraction ρ_n^x vanishes at low temperature, the second sound velocity will diverge as $T \rightarrow 0$ and the mode becomes ill-defined.

The results above also allow to compare the superfluid smectic phase with two quite different examples that exhibit a similar symmetry breaking pattern. As discussed in Sec. III B, the superfluid smectic realizes two independent broken $U(1)$ symmetries that are associated with the thermodynamic variables \mathbf{v}_s and ∇u in Eq. (51). The superfluid velocity $\mathbf{v}_s = (\hbar/m)\nabla\theta_{\text{sf}}$ may be derived from an angular variable $\theta_{\text{sf}} \in (-\pi, \pi]$. Moreover, since $q_0 u(x, y)$ and $q_0 u(x, y) + 2\pi$ give rise to identical distortions of the smectic order [cf. Eq. (49)], the same type of symmetry breaking characterizes a smectic phase. Its fluctuations may thus be described by a different angle $\theta_{\text{sm}} \in (-\pi, \pi]$ such that $\nabla u = (1/q_0)\nabla\theta_{\text{sm}}$ [90]. As pointed out by Radzihovsky and Vishwanath [81], these symmetry-breaking variables also appear in a Larkin-Ovchinnikov phase of an imbalanced Fermi superfluid, where the mismatch $q_0 = k_{F\uparrow} - k_{F\downarrow}$ of the two Fermi surfaces results in an uni-directional periodic modulation of the complex gap parameter Δ_{q_0} . The associated low energy theory derived by these authors and discussed in much more detail in Ref. [82] is of the form

$$\mathcal{H}_{\text{LO}} = \frac{K_1}{2} (\nabla^2 u)^2 + \frac{B}{2} \left(\partial_{\parallel} u - \frac{1}{2} (\nabla u)^2 \right)^2 + \frac{\rho_s^i}{2} (\nabla_i \theta_{\text{sf}})^2 \quad (\text{C20})$$

where $i = \parallel$ or $i = \perp$ refer to the directions parallel and transverse to the ordering vector. The two Goldstone modes associated with the Hamiltonian density (C20) are determined by the elastic constants K_1 and B together with the two different superfluid densities ρ_s^{\perp} and ρ_s^{\parallel} and a finite compressibility χ in the form

$$\omega_{\text{sf}}(\mathbf{q}) = \sqrt{(\rho_s^{\perp} q_{\perp}^2 + \rho_s^{\parallel} q_{\parallel}^2)/\chi} \quad (\text{C21})$$

$$\omega_{\text{sm}}(\mathbf{q}) = \sqrt{(K_1 q_{\perp}^4 + B q_{\parallel}^2)/\chi}. \quad (\text{C22})$$

The first mode is an anisotropic version of the Bogoliubov-Anderson mode of a neutral superfluid while the smectic phonon $\omega_{\text{sm}}(\mathbf{q})$ is unique for the uni-directional LO state. It has a linear spectrum determined by the layer compression modulus B for wave vectors along the direction of ordering but turns into a mode with quadratic dispersion for $\mathbf{q} \perp \mathbf{q}_0$. The predicted mode structure differs from that of the superfluid smectic phase discussed above and indeed there are important differences between both phases. First of all, the uni-directional LO state only exists in the superfluid

regime of the imbalanced Fermi gas. The elastic constants B and K_1 therefore derive from a single complex order parameter Δ_{q_0} . Moreover, in contrast to the superfluid smectic phase of dipolar BECs, it is assumed that the spatial structure in Δ_{q_0} is not associated with a real density modulation and also that the fermionic superfluid has no underlying zero-momentum condensate. These assumptions are valid for essentially incompressible Fermi systems in the BCS limit, where the condensate fraction is exponentially small. They imply that there is no coupling of the symmetry breaking variables ∇u and \mathbf{v}_s to the particle and momentum density. The energy density (C20) associated with ∇u and \mathbf{v}_s thus fully determines the spectrum of Goldstone modes [91].

By contrast, the equations of motion (C15) that determine the hydrodynamic modes of a superfluid smectic phase depend crucially on the coupling between density fluctuations $\delta\rho$ and both symmetry-breaking variables. Different from the LO phase of an incompressible superfluid Fermi system, it is thus a true supersolid in the sense of showing dissipationless transport of particles. This point can be illustrated by using an approach due to Yoo and Dorsey [86]. They decompose small fluctuations of the mass density (suppressing the superscript y in the following for the longitudinal direction)

$$\delta\rho = -\rho u' + \delta\rho_\Delta \quad (\text{C23})$$

into a contribution $-\rho u'$ associated with deformations of the periodic structure and an additional defect density ρ_Δ . It obeys a continuity equation

$$\partial_t \delta\rho_\Delta = -\partial_y \rho_s (v_s - v_n), \quad (\text{C24})$$

where the associated conserved current $g_\Delta = \rho_s (v_s - v_n)$ is just the Galilei invariant superfluid mass current density, which is determined by the counterflow between the superfluid and the normal velocity $v_n = \partial_t u$. To re-derive our results for the sound modes, it is convenient to consider the second time derivative of the continuity equation for the defect density, which reads

$$\partial_t^2 \delta\rho_\Delta = \rho_s \partial_y^2 (\mu/m) + \rho_s \partial_t^2 u'. \quad (\text{C25})$$

This equation for the longitudinal propagation is a special case of the hydrodynamic equations for supersolids first derived by Andreev and Lifshitz [92]. For the superfluid smectic with a small density modulation, the contributions which involve the layer phase variable u'

may be neglected to leading order. In this limit, the velocity is given by the result $c_4^2 = f_s (K/\rho)$ characteristic of a fourth sound mode, which describes the oscillation of the dominant superfluid component with no motion of the lattice. In general, as Eq. (C25) shows, the defect density and the longitudinal strain u' are coupled. An explicit result for the eigenmodes of a supersolid thus requires to simultaneously solve the equation for $\delta\rho_\Delta$ and for u' , which reads

$$\rho_n \partial_t^2 u' = \partial_y^2 [-p + B u' + \rho_s (\mu/m)]. \quad (\text{C26})$$

The solution of these coupled equations does — of course — reproduce our result (63), where now the corresponding dimensionless eigenvectors are $(\delta\rho_\Delta/\rho, u') = (c_2^2/(K/\rho), 1)$ for the first sound mode with speed c_1 and $(\delta\rho_\Delta/\rho, u') = (c_1^2/(K/\rho), 1)$ for the second sound mode with speed c_2 . In the limit $B/\rho_n \ll K/\rho$, the compression mode with speed c_1 does not involve an oscillation of the defect density and only contains the layer phase variable, which means that the density variation in this sound mode is solely due to changes in the periodic structure of the smectic. In the same limit, the second sound mode contains both an oscillation in the longitudinal strain as well as the defect density, which describes density transport independent of variations in the smectic lattice structure.

A second example where superfluidity appears simultaneously with a periodic density modulation along a single direction is provided by the stripe phase of BECs in the presence of spin-orbit coupling. The momentum transfer associated with the Raman coupling between two internal states may then lead to a density modulation of the type assumed in Eq. (48) with wave vector $q_0 = 2k_1$. In particular, the amplitude n_1 may be tuned by the strength Ω of the Raman coupling [93]. The role of the layer phase variable u is played by the relative phase ϕ between the complex coefficients C_1 and C_2 in the Gross-Pitaevskii ansatz [93]

$$\begin{pmatrix} \psi_a \\ \psi_b \end{pmatrix} = \sqrt{\frac{N}{V}} \left[C_1 \begin{pmatrix} \cos \theta \\ -\sin \theta \end{pmatrix} e^{ik_1 x} + C_2 \begin{pmatrix} \sin \theta \\ -\cos \theta \end{pmatrix} e^{-ik_1 x} \right] \quad (\text{C27})$$

for the spinor wave function, where θ is a variational parameter. Expanding the resulting energy density $\varepsilon(k_1)$ to quadratic order around the optimum value of the wave vector k_1 will give rise to a finite elastic contribution $f_{\text{el}} = \tilde{B} (\nabla\phi)^2/2 + \dots$ to the free energy density, where \tilde{B} plays the role of an effective layer compression modulus. The stripe phase is thus expected to behave in an analogous manner as the superfluid smectic phase of dipolar gases discussed here. A detailed analysis of this problem is left for future investigation.

[1] V. V. Flambaum, G. F. Gribakin, and C. Harabati, “Analytical calculation of cold-atom scattering,” *Phys. Rev. A* **59**, 1998 (1999).

[2] S. Tan, “Energetics of a strongly correlated Fermi gas,” *Annals of Physics* **323**, 2952 (2008).

[3] S. Tan, “Large momentum part of a strongly correlated

- Fermi gas,” *Annals of Physics* **323**, 2971 (2008).
- [4] S. Tan, “Generalized virial theorem and pressure relation for a strongly correlated Fermi gas,” *Annals of Physics* **323**, 2987 (2008).
- [5] S. Zhang and A. J. Leggett, “Universal properties of the ultracold Fermi gas,” *Phys. Rev. A* **79**, 023601 (2009).
- [6] E. Braaten and L. Platter, “Exact Relations for a Strongly Interacting Fermi Gas from the Operator Product Expansion,” *Phys. Rev. Lett.* **100**, 205301 (2008).
- [7] E. Braaten, “Universal Relations for Fermions with Large Scattering Length,” in *The BCS–BEC Crossover and the Unitary Fermi Gas*, edited by W. Zwerger (Springer, Heidelberg, 2012).
- [8] C. Chin, R. Grimm, P. Julienne, and E. Tiesinga, “Feshbach resonances in ultracold gases,” *Rev. Mod. Phys.* **82**, 1225 (2010).
- [9] E. Braaten and H.-W. Hammer, “Universality in few-body systems with large scattering length,” *Physics Reports* **428**, 259 (2006).
- [10] A. Griesmaier, J. Werner, S. Hensler, J. Stuhler, and T. Pfau, “Bose-Einstein Condensation of Chromium,” *Phys. Rev. Lett.* **94**, 160401 (2005).
- [11] M. Lu, S. H. Youn, and B. L. Lev, “Trapping Ultracold Dysprosium: A Highly Magnetic Gas for Dipolar Physics,” *Phys. Rev. Lett.* **104**, 063001 (2010).
- [12] M. Lu, N. Q. Burdick, and B. L. Lev, “Quantum Degenerate Dipolar Fermi Gas,” *Phys. Rev. Lett.* **108**, 215301 (2012).
- [13] K. Aikawa, A. Frisch, M. Mark, S. Baier, A. Rietzler, R. Grimm, and F. Ferlaino, “Bose-Einstein Condensation of Erbium,” *Phys. Rev. Lett.* **108**, 210401 (2012).
- [14] K. Aikawa, A. Frisch, M. Mark, S. Baier, R. Grimm, and F. Ferlaino, “Reaching Fermi Degeneracy via Universal Dipolar Scattering,” *Phys. Rev. Lett.* **112**, 010404 (2014).
- [15] T. Takekoshi, L. Reichsöllner, A. Schindewolf, J. M. Hutson, C. R. Le Sueur, O. Dulieu, F. Ferlaino, R. Grimm, and H.-C. Nägerl, “Ultracold Dense Samples of Dipolar RbCs Molecules in the Rovibrational and Hyperfine Ground State,” *Phys. Rev. Lett.* **113**, 205301 (2014).
- [16] P. K. Molony, P. D. Gregory, Z. Ji, B. Lu, M. P. Köpinger, C. R. Le Sueur, C. L. Blackley, J. M. Hutson, and S. L. Cornish, “Creation of Ultracold $^{87}\text{Rb}^{133}\text{Cs}$ Molecules in the Rovibrational Ground State,” *Phys. Rev. Lett.* **113**, 255301 (2014).
- [17] J. W. Park, S. A. Will, and M. W. Zwierlein, “Ultracold Dipolar Gas of Fermionic $^{23}\text{Na}^{40}\text{K}$ Molecules in Their Absolute Ground State,” *Phys. Rev. Lett.* **114**, 205302 (2015).
- [18] F. Böttcher, J.-N. Schmidt, M. Wenzel, J. Hertkorn, M. Guo, T. Langen, and T. Pfau, “Transient Supersolid Properties in an Array of Dipolar Quantum Droplets,” *Phys. Rev. X* **9**, 011051 (2019).
- [19] L. Tanzi, E. Lucioni, F. Famà, J. Catani, A. Fioretti, C. Gabbanini, R. N. Bisset, L. Santos, and G. Modugno, “Observation of a Dipolar Quantum Gas with Metastable Supersolid Properties,” *Phys. Rev. Lett.* **122**, 130405 (2019).
- [20] L. Chomaz, D. Petter, P. Ilzhöfer, G. Natale, A. Trautmann, C. Politi, G. Durastante, R. M. W. van Bijnen, A. Patscheider, M. Sohmen, M. J. Mark, and F. Ferlaino, “Long-Lived and Transient Supersolid Behaviors in Dipolar Quantum Gases,” *Phys. Rev. X* **9**, 021012 (2019).
- [21] A. M. Perelomov and V. S. Popov, ““Fall to the center” in quantum mechanics,” *Theoretical and Mathematical Physics* **4**, 664 (1970).
- [22] L. D. Landau and E. M. Lifshitz, *Quantum Mechanics: Non-relativistic Theory* (Pergamon Press, 1965), Eq. (123.2)
- [23] Y. Wang, Julianne. P., and C. H. Greene, “Few-body physics of ultracold atoms and molecules with long-range interactions,” in *Annual Review of Cold Atoms and Molecules* (2014) Chap. 2.
- [24] M. E. Fisher, “The free energy of a macroscopic system,” *Archive for Rational Mechanics and Analysis* **17**, 377 (1964).
- [25] H. P. Büchler, E. Demler, M. Lukin, A. Micheli, N. Prokof’ev, G. Pupillo, and P. Zoller, “Strongly Correlated 2D Quantum Phases with Cold Polar Molecules: Controlling the Shape of the Interaction Potential,” *Phys. Rev. Lett.* **98**, 060404 (2007).
- [26] D. S. Fisher and P. C. Hohenberg, “Dilute Bose gas in two dimensions,” *Phys. Rev. B* **37**, 4936 (1988).
- [27] B. Spivak and S. A. Kivelson, “Phases intermediate between a two-dimensional electron liquid and Wigner crystal,” *Phys. Rev. B* **70**, 155114 (2004).
- [28] C. Ticknor, “Two-dimensional dipolar scattering,” *Phys. Rev. A* **80**, 052702 (2009).
- [29] H. Friedrich, *Scattering Theory* (Springer (Berlin), 2013).
- [30] F. G. Giuliani and G. Vignale, *Quantum Theory of the Electron Liquid* (Cambridge University Press, 2005).
- [31] S. K. Adhikari, “Quantum scattering in two dimensions,” *American Journal of Physics* **54**, 362 (1986).
- [32] F. Arnecke, H. Friedrich, and P. Raab, “Near-threshold scattering, quantum reflection, and quantization in two dimensions,” *Phys. Rev. A* **78**, 052711 (2008).
- [33] The breakdown of the effective-range expansion is apparent from a divergence in the Bethe integral expression for the scattering phase shift when evaluated using the dipolar two-body wave function at threshold (5) [32, 94]. The correction in Eq. (4) is obtained by regulating this divergence with an upper cutoff of order $1/k$.
- [34] I. Bloch, J. Dalibard, and W. Zwerger, “Many-body physics with ultracold gases,” *Rev. Mod. Phys.* **80**, 885 (2008).
- [35] W. M. Frank, D. J. Land, and R. M. Spector, “Singular Potentials,” *Rev. Mod. Phys.* **43**, 36 (1971).
- [36] K. M. Case, “Singular Potentials,” *Phys. Rev.* **80**, 797 (1950).
- [37] J. Hofmann, “Current response, structure factor and hydrodynamic quantities of a two- and three-dimensional Fermi gas from the operator-product expansion,” *Phys. Rev. A* **84**, 043603 (2011).
- [38] W. D. Goldberger and I. Z. Rothstein, “Structure-function sum rules for systems with large scattering lengths,” *Phys. Rev. A* **85**, 013613 (2012).
- [39] J. Hofmann, M. Barth, and W. Zwerger, “Short-distance properties of Coulomb systems,” *Phys. Rev. B* **87**, 235125 (2013).
- [40] F. Werner and Y. Castin, “General relations for quantum gases in two and three dimensions: Two-component fermions,” *Phys. Rev. A* **86**, 013626 (2012).
- [41] F. Werner and Y. Castin, “General relations for quantum gases in two and three dimensions. II. Bosons and mixtures,” *Phys. Rev. A* **86**, 053633 (2012).
- [42] P. J. Price, “Density Fluctuations at Low Temperatures,” *Phys. Rev.* **94**, 257 (1954).
- [43] M. Barth and J. Hofmann, “Efimov correlations in

- strongly interacting Bose gases,” *Phys. Rev. A* **92**, 062716 (2015).
- [44] V. N. Popov, “On the theory of the superfluidity of two- and one-dimensional bose systems,” *Theoretical and Mathematical Physics* **11**, 565 (1972).
- [45] M. Schick, “Two-Dimensional System of Hard-Core Bosons,” *Phys. Rev. A* **3**, 1067 (1971).
- [46] C. Mora and Y. Castin, “Ground State Energy of the Two-Dimensional Weakly Interacting Bose Gas: First Correction Beyond Bogoliubov Theory,” *Phys. Rev. Lett.* **102**, 180404 (2009).
- [47] G. E. Astrakharchik, J. Boronat, J. Casulleras, I. L. Kurbakov, and Yu. E. Lozovik, “Equation of state of a weakly interacting two-dimensional Bose gas studied at zero temperature by means of quantum Monte Carlo methods,” *Phys. Rev. A* **79**, 051602 (2009).
- [48] J. Hofmann and W. Zwerger, unpublished.
- [49] M. Valiente, N. T. Zinner, and K. Mølmer, “Universal relations for the two-dimensional spin-1/2 Fermi gas with contact interactions,” *Phys. Rev. A* **84**, 063626 (2011).
- [50] J. Hofmann, “Quantum Anomaly, Universal Relations, and Breathing Mode of a Two-Dimensional Fermi Gas,” *Phys. Rev. Lett.* **108**, 185303 (2012).
- [51] F. Werner, “Virial theorems for trapped cold atoms,” *Phys. Rev. A* **78**, 025601 (2008).
- [52] K. Góral, B.-G. Englert, and K. Rzażewski, “Semiclassical theory of trapped fermionic dipoles,” *Phys. Rev. A* **63**, 033606 (2001).
- [53] M. S. Wertheim, “Exact Solution of the Mean Spherical Model for Fluids of Hard Spheres with Permanent Electric Dipole Moments,” *The Journal of Chemical Physics* **55**, 4291 (1971).
- [54] J.-P. Hansen and I. R. McDonald, *Theory of Simple Liquids* (Academic Press, 2006).
- [55] M. Barth and W. Zwerger, “Tan relations in one dimension,” *Annals of Physics* **326**, 2544 (2011).
- [56] M. Valiente, N. T. Zinner, and K. Mølmer, “Universal properties of Fermi gases in arbitrary dimensions,” *Phys. Rev. A* **86**, 043616 (2012).
- [57] G. E. Astrakharchik, J. Boronat, I. L. Kurbakov, and Yu. E. Lozovik, “Quantum Phase Transition in a Two-Dimensional System of Dipoles,” *Phys. Rev. Lett.* **98**, 060405 (2007).
- [58] B. Spivak and S. A. Kivelson, “Transport in two dimensional electronic micro-emulsions,” *Annals of Physics* **321**, 2071 (2006).
- [59] N. R. Cooper, E. H. Rezayi, and S. H. Simon, “Vortex Lattices in Rotating Atomic Bose Gases with Dipolar Interactions,” *Phys. Rev. Lett.* **95**, 200402 (2005).
- [60] S. Komineas and N. R. Cooper, “Vortex lattices in Bose-Einstein condensates with dipolar interactions beyond the weak-interaction limit,” *Phys. Rev. A* **75**, 023623 (2007).
- [61] J.-P. Hansen and L. Verlet, “Phase Transitions of the Lennard-Jones System,” *Phys. Rev.* **184**, 151 (1969).
- [62] M. Babadi, B. Skinner, M. M. Fogler, and E. Demler, “Universal behavior of repulsive two-dimensional fermions in the vicinity of the quantum freezing point,” *EPL (Europhysics Letters)* **103**, 16002 (2013).
- [63] M. H. Kalos, D. Levesque, and L. Verlet, “Helium at zero temperature with hard-sphere and other forces,” *Phys. Rev. A* **9**, 2178 (1974).
- [64] D. Petter, G. Natale, R. M. W. van Bijnen, A. Patscheider, M. J. Mark, L. Chomaz, and F. Ferlaino, “Probing the Roton Excitation Spectrum of a Stable Dipolar Bose Gas,” *Phys. Rev. Lett.* **122**, 183401 (2019).
- [65] D. J. Griffiths, “Hyperfine splitting in the ground state of hydrogen,” *American Journal of Physics* **50**, 698 (1982).
- [66] L. Santos, G. V. Shlyapnikov, and M. Lewenstein, “Roton-Maxon Spectrum and Stability of Trapped Dipolar Bose-Einstein Condensates,” *Phys. Rev. Lett.* **90**, 250403 (2003).
- [67] D. H. J. O’Dell, S. Giovanazzi, and G. Kurizki, “Rotons in Gaseous Bose-Einstein Condensates Irradiated by a Laser,” *Phys. Rev. Lett.* **90**, 110402 (2003).
- [68] D. M. Ceperley, “Path integrals in the theory of condensed helium,” *Rev. Mod. Phys.* **67**, 279 (1995).
- [69] U. R. Fischer, “Stability of quasi-two-dimensional Bose-Einstein condensates with dominant dipole-dipole interactions,” *Phys. Rev. A* **73**, 031602 (2006).
- [70] A. R. P. Lima and A. Pelster, “Quantum fluctuations in dipolar Bose gases,” *Phys. Rev. A* **84**, 041604 (2011).
- [71] Z.-K. Lu, Y. Li, D. S. Petrov, and G. V. Shlyapnikov, “Stable Dilute Supersolid of Two-Dimensional Dipolar Bosons,” *Phys. Rev. Lett.* **115**, 075303 (2015).
- [72] P. B. Blakie, D. Baillie, and R. N. Bisset, “Roton spectroscopy in a harmonically trapped dipolar Bose-Einstein condensate,” *Phys. Rev. A* **86**, 021604 (2012).
- [73] J. Hofmann and W. Zwerger, “Deep Inelastic Scattering on Ultracold Gases,” *Phys. Rev. X* **7**, 011022 (2017).
- [74] F. Mazzanti, R. E. Zillich, G. E. Astrakharchik, and J. Boronat, “Dynamics of a Two-Dimensional System of Quantum Dipoles,” *Phys. Rev. Lett.* **102**, 110405 (2009).
- [75] D. Petter, A. Patscheider, G. Natale, M. J. Mark, M. A. Baranov, R. v. Bijnen, S. M. Roccuzzo, A. Recati, B. Blakie, D. Baillie, L. Chomaz, and F. Ferlaino, “High-energy Bragg scattering measurements of a dipolar supersolid,” arXiv:2005.02213 (2020).
- [76] P. M. Chaikin and T. C. Lubensky, *Principles of condensed matter physics* (Cambridge University Press, 1995).
- [77] P. C. Martin, O. Parodi, and P. S. Pershan, “Unified Hydrodynamic Theory for Crystals, Liquid Crystals, and Normal Fluids,” *Phys. Rev. A* **6**, 2401 (1972).
- [78] G. Natale, R. M. W. van Bijnen, A. Patscheider, D. Petter, M. J. Mark, L. Chomaz, and F. Ferlaino, “Excitation Spectrum of a Trapped Dipolar Supersolid and Its Experimental Evidence,” *Phys. Rev. Lett.* **123**, 050402 (2019).
- [79] L. Tanzi, S. M. Roccuzzo, E. Lucioni, F. Famà, A. Fioretti, C. Gabbanini, G. Modugno, A. Recati, and S. Stringari, “Supersolid symmetry breaking from compressional oscillations in a dipolar quantum gas,” *Nature* **574**, 382 (2019).
- [80] M. Guo, F. Böttcher, J. Hertkorn, J.-N. Schmidt, M. Wenzel, H. P. Büchler, T. Langen, and T. Pfau, “The low-energy Goldstone mode in a trapped dipolar supersolid,” *Nature* **574**, 386 (2019).
- [81] L. Radzihovsky and A. Vishwanath, “Quantum Liquid Crystals in an Imbalanced Fermi Gas: Fluctuations and Fractional Vortices in Larkin-Ovchinnikov States,” *Phys. Rev. Lett.* **103**, 010404 (2009).
- [82] L. Radzihovsky, “Fluctuations and phase transitions in Larkin-Ovchinnikov liquid-crystal states of a population-imbalanced resonant Fermi gas,” *Phys. Rev. A* **84**, 023611 (2011).
- [83] D. T. Son, “Effective Lagrangian and Topological Interactions in Supersolids,” *Phys. Rev. Lett.* **94**, 175301

- (2005).
- [84] A. J. Leggett, “Can a solid be ”superfluid”?” Phys. Rev. Lett. **25**, 1543 (1970).
- [85] If irreversible effects are included, the right-hand side in this equation no longer vanishes and contains a contribution $\zeta \nabla^2 h$, where ζ is the dissipative coefficient that enters the diffusion constant $D_p = \zeta B$ of the permeation mode [76].
- [86] C.-D. Yoo and A. T. Dorsey, “Hydrodynamic theory of supersolids: Variational principle, effective Lagrangian, and density-density correlation function,” Phys. Rev. B **81**, 134518 (2010).
- [87] S. Sacconi, S. Moroni, and M. Boninsegni, “Excitation Spectrum of a Supersolid,” Phys. Rev. Lett. **108**, 175301 (2012).
- [88] This result cannot remain valid beyond mean-field theory since it would predict a finite second sound velocity c_2 even at the transition to the fluid phase. The layer compression modulus $B \sim |n_1|^x$ must therefore vanish with an exponent $x > 2$. In fact, as was shown by Grinstein and Pelcovits [95], the renormalized value B_{ren} vanishes at long distances even in the smectic phase with $n_1 \neq 0$ due to anharmonic corrections to the linear elastic continuum model used above. In the following, this complication will be ignored.
- [89] The fact that to leading order in the velocities, the pressure will not depend on the superfluid velocity or the layer phase gradient follows from our definition of \mathbf{h} and \mathbf{j}_s in combination with Maxwell relations that link \mathbf{h} and the pressure, which can be derived from the thermodynamic differential $d\tilde{\varepsilon} = Td\tilde{s} - pd(1/\rho) + \mathbf{v}_n d(\mathbf{j}/\rho) + (\mathbf{j}_s/\rho)d\mathbf{v}_s + (\mathbf{h}_u/\rho)d\mathbf{v}_u$ for the energy per particle $\tilde{\varepsilon} = \varepsilon/\rho$.
- [90] The formal analogy of the order in smectic A liquid crystals and in superfluids was realized by de Gennes [96]. Note that the associated angles θ_{sm} and θ_{sf} transform in an opposite manner under time reversal: θ_{sm} is a true scalar while θ_{sf} is a pseudoscalar.
- [91] It is interesting to note that the number of Goldstone modes is reduced to only one in a Fulde-Ferrell phase with uni-directional order. In this case, time-reversal symmetry is broken and there is only a single contribution $(\rho_s/2)(\hat{\mathbf{q}}_0 \cdot \mathbf{v}_s - (\hbar q_0/m)\partial_{\parallel} u)^2$ to the free energy density rather than two independent ones associated with superfluid flow and elastic distortions. The Fulde-Ferrell state therefore realizes a broken relative gauge symmetry as in $^3\text{He A}$ [97].
- [92] A. F. Andreev and I. M. Lifshitz, “Quantum Theory of Defects in Crystals,” JETP **29**, 1107 (1969).
- [93] Y. Li, L. P. Pitaevskii, and S. Stringari, “Quantum Tricriticality and Phase Transitions in Spin-Orbit Coupled Bose-Einstein Condensates,” Phys. Rev. Lett. **108**, 225301 (2012).
- [94] H. A. Bethe, “Theory of the Effective Range in Nuclear Scattering,” Phys. Rev. **76**, 38 (1949).
- [95] G. Grinstein and R. A. Pelcovits, “Anharmonic Effects in Bulk Smectic Liquid Crystals and Other ”One-Dimensional Solids”,” Phys. Rev. Lett. **47**, 856 (1981).
- [96] P. G. de Gennes, “An analogy between superconductors and smectics A,” Solid State Communications **10**, 753 (1972).
- [97] A. J. Leggett, “A theoretical description of the new phases of liquid ^3He ,” Rev. Mod. Phys. **47**, 331 (1975).